12-17-2010

An Underwater Channel Model and Chirp Slope Keying Modulation Scheme Performance

Brice Zoh
University of New Orleans

An Underwater Channel Model and Chirp Slope Keying Modulation Scheme Performance

A Thesis

Submitted to the Graduate Faculty of the
University of New Orleans
in partial fulfillment of the
requirements for the Degree of

Master of Science
in
Engineering
Electrical

by

Brice Zoh

B.S. University of New Orleans, 2008
December, 2010

ACKNOWLEDGMENTS

I am deeply grateful to my thesis advisor Dr. Edit K. Bourgeois for steadily helping, guiding and assisting me all these months. She has undoubtedly been a crucial architect in the development of this research.

I thank all my professors, classmates, and friends for their immense contribution to my education.

I specifically express my sincere gratitude to Dr.Rasheed Azzam for believing in me and giving me the opportunity to become a better engineer.

My greatest appreciation goes to God and my family, especially my mother Holle Celestine for her support and immeasurable love. Mom, you have been and remain my source of inspiration.

ABSTRACT

Chirp-Slope Keying (CSK) is a new and innovative digital modulation scheme for underwater data transmission. The underwater environment brings up several challenges to the manufacturing and operation of communication systems. This thesis shows through analysis and simulations the effectiveness of Chirp-Slope Keying (CSK) in providing a satisfying performance in underwater communication. The experiment consists of modulating a chirp slope by binary numbers (representing our data). '0' is represented by a linear- down chirp and '1' is represented by a linear-up chirp . The received data is first processed by a correlator receiver. Then, the detection of either binary symbol is obtained by the comparison to a threshold. Simulation results for numerous signal-to-noise ratios show that CSK provides satisfying performance for underwater data transmission.

The Mississippi gulf coast shallow water Data collected from the National Oceanic and Atmospheric Administration (NOAA), (see appendix), allow us to accurately generate a laboratory model for the channel of interest.

Keywords: Engineering, Southeastern United States, Signal Processing

TABLE OF CONTENTS

LIST OF FIGURES

LIST OF TABLES

1. INTRODUCTION

Communications play a central role in our lives. It is important for humans to be able to interact with each other. Even if communications techniques in the air have been perfected, they are still lagging in the underwater environment. This is mainly due to numerous factors that will be enumerated in what follows.

1.1 CHALLENGES OF UNDERWATER COMMUNICATION

Today, many underwater devices communicate through the means of cables. Although these channels, mostly fiber optics, offer an acceptable performance, they have several limitations which make their use difficult in some situations. In fact, they are unpractical for moving targets, the cost of maintenance is high and repair tasks can be very difficult if the transducers are located in deep waters.

These drawbacks have inevitably imposed the development of other communication techniques. Acoustic wireless transmission is the best suited method for Underwater Wireless Communications (UWC). UWC are constituted by devices such as sensors and Underwater Autonomous Vehicles (UAVs) that interact to collaboratively share data and applications over a certain distance and a given environment. Underwater Acoustic Communication presents various challenges due to the characteristics of the water channel. Countless effects such as fading, ambient noise, absorption, multipath and refractive properties of sound, and Doppler spreading impose the need to design and implement better modulation schemes. The use of Chirp-Slope Keying (CSK) provides acceptable data communication performance in nature most

unforgiving medium. This thesis gives a very brief introduction to wireless communications as well as Chirp-Slope Keying (CSK). It also provides information on how to model the underwater channel. Finally, simulation results are analyzed and future research challenges are discussed.

1.2 THESIS OUTLINE

For a better and thorough understanding of the work done and presented herein, this thesis is structured as follows: In Chapter 2, we explain the basics of underwater signal propagation. Our focus is on major channel flaws such as transmission loss and ambient noise in shallow water. The statistical characteristics of the underwater channel model are introduced in Chapter 3.

Chapter 4 gives a detailed explanation of chirp slope keying modulation (CSK). Theoretical and general properties as well as mathematical representation are outlined. System description is presented in Chapter 5 and simulation results for various underwater conditions are presented in Chapter 6. Finally; Chapter 7 discusses the research challenges of underwater channels and concludes the thesis by providing suggestions for future work.

2. PROPAGATION OF SOUND IN THE OCEAN

The understanding of sound propagation in the sea is an important step toward developing reliable underwater acoustic communication schemes. In fact, the physical and chemical properties of sea water affect the propagation of sound underwater. Communication channels in the sea are characterized by a path loss that depends not only on the distance between the transmitter and the receiver but also on the signal frequency [2-3].In addition, the presence of impairments in the medium creates a non-negligible source of noise. These two factors are the main causes of limitations on Signal-to-Noise Ratio (SNR) and therefore performance. Other phenomena such as reverberation, scattering and Doppler effects contribute also to system performance limitations [3].

2.1 TRANSMISSION LOSS

The transmission loss reduces the intensity of sound traveling from the transmitter to the receiver. An analysis of transmission loss is necessary to understand how sound signal propagates underwater. Our research area focuses on shallow water. We therefore use data collected from the National Oceanic and Atmospheric Administration (NOOA), presented in appendix E, to produce simple models of shallow water channels. The magnitude of sonar transmission loss may be estimated by summing up the effects of geometrical spreading, absorption and scattering, as appropriate, those are frequency dependent and therefore limit our range of frequency.

Spreading occurs when the sound signal loses intensity as it spreads outwards from the emitting source. Absorption, on the other hand, happens when the acoustic energy is converted into heat. Scattering is defined as the redirection of sound waves as they collide with obstacles.

2.1.1 SIGNAL SPREADING

The transmission of sound in the ocean can either be cylindrical or spherical. In shallow water, the spreading is exclusively cylindrical [1]. Transmission loss (Tl), in dB, is given by [1]:

$$\mathrm{Tl} = 10\log \mathrm{r} + 10^{-3}\alpha \mathrm{r}\ , \qquad (2.1)$$

where r represents the distance between the transmitter and the receiver in km, and α is the absorption coefficient in dB/km. Our expected range of transmission is 1km, so equation (2.1) becomes :

$$\mathrm{Tl} = 10^{-3}\alpha\ . \qquad (2.2)$$

2.1.2 SIGNAL ABSORPTION

Sound is attenuated underwater due to the presence of chemical components [3]. To ensure minimal signal absorption, we have chosen the frequency range from 5 kHz to 15 kHz. For that band of frequencies, the elements favoring signal attenuation are boric acid and magnesium sulfate [3]. Viscous attenuation does not participate in the

signal attenuation because it is only significant at very high frequency (above 100 kHz) [3]. Numerous factors and properties of sea water such as acoustic frequency, pressure, acidity, temperature and salinity, play a major role in the characterization of the absorption coefficient expression. The absorption coefficient, in dB/Km, is [3]:

$$\alpha = \left(\frac{\mathrm{A_1 P_1} f_1}{f^2 + f_1^2} + \frac{\mathrm{A_2 P_2} f_2}{f^2 + f_2^2} + \mathrm{A_3 P_3}\right) f^2, \qquad (2.3)$$

where f represents the frequency, in kHz, of the sound wave being transmitted over the channel.

A_1 is the boric acid component in sea water and is given by [3]:

$$\mathrm{A_1} = \frac{8.68}{\mathrm{c}}\, 10^{(0.78\mathrm{pH}-5)}, \qquad (2.4)$$

where pH is the ph of sea water. Equation 2.5 gives the speed of sound underwater (c) in m/s [11]:

$$\mathrm{c} = 1412 + 3.21\,\mathrm{T} + 1.19\,\mathrm{S} + 0.0167\,\mathrm{z}\,, \qquad (2.5)$$

T is the temperature of the water (in degrees Celsius), S is the salinity in mg/l, and z is the depth in meters.

$\mathrm{P_1}$, in (2.3), is the depth pressure of boric acid in sea water. Its normalized value for shallow waters as given by [11] is 1 Pa.

Boric acid relaxation frequency is denoted by f_1 (in kHz) in (2.3), and is given by [11]:

$$f_1 = 2.8\left(\frac{\mathrm{S}}{35}\right)^{\frac{1}{2}}\, 10^{\left(4-\frac{1245}{(273+\mathrm{T})}\right)}, \qquad (2.6)$$

magnesium sulfate relaxation frequency f_2 (in kHz) is given by [11]:

$$f_2 = \frac{8.17}{1+0.0018(\mathrm{S}-35)}\ 10^{\left(8-\frac{1990}{273+\mathrm{T}}\right)}, \qquad (2.\ 7)$$

A_2 , the magnesium sulfate component is expressed as [11]:

$$\mathrm{A}_2 = 21.44\ \left(\frac{\mathrm{S}}{\mathrm{c}}\right)(1 + 0.025\mathrm{T}), \qquad (2.8)$$

P_2 (in Pa) is the depth pressure for magnesium sulfate [11]:

$$\mathrm{P}_2 = 1 - 1.37\ \mathrm{x}\ 10^{-4}\mathrm{z} + 6.2\ \mathrm{x}\ 10^{-9}\mathrm{z}^2, \qquad (2.9)$$

pure water component in the sea (A_3) is given by [11]:

$$\mathrm{A}_3 = 3.964\ \mathrm{x}\ 10^{-4} - 1.146\ \mathrm{x}\ 10^{-5}\mathrm{T} + \ 1.45\ \mathrm{x}\ 10^{-7}\mathrm{T}^2 - 6.5\ \mathrm{x}\ 10^{-10}\mathrm{T}^3, \qquad (2.10)$$

pure water depth pressure is P_3 (in Pa) and is given by [11]:

$$\mathrm{P}_3 = \ 1 - 3.83\ \mathrm{x}\ 10^{-5}\mathrm{z} + 4.9\ \mathrm{x}\ 10^{-10}\mathrm{z}^2\ . \qquad (2.11)$$

The absorption coefficient variation, shown in Figure 2.1, is a function of frequency. As the frequency increases, so does the absorption. This limits the range of frequencies for which data can be transmitted underwater. This is one of the reasons why we will be using the frequency range from 5 kHz to 15 kHz.

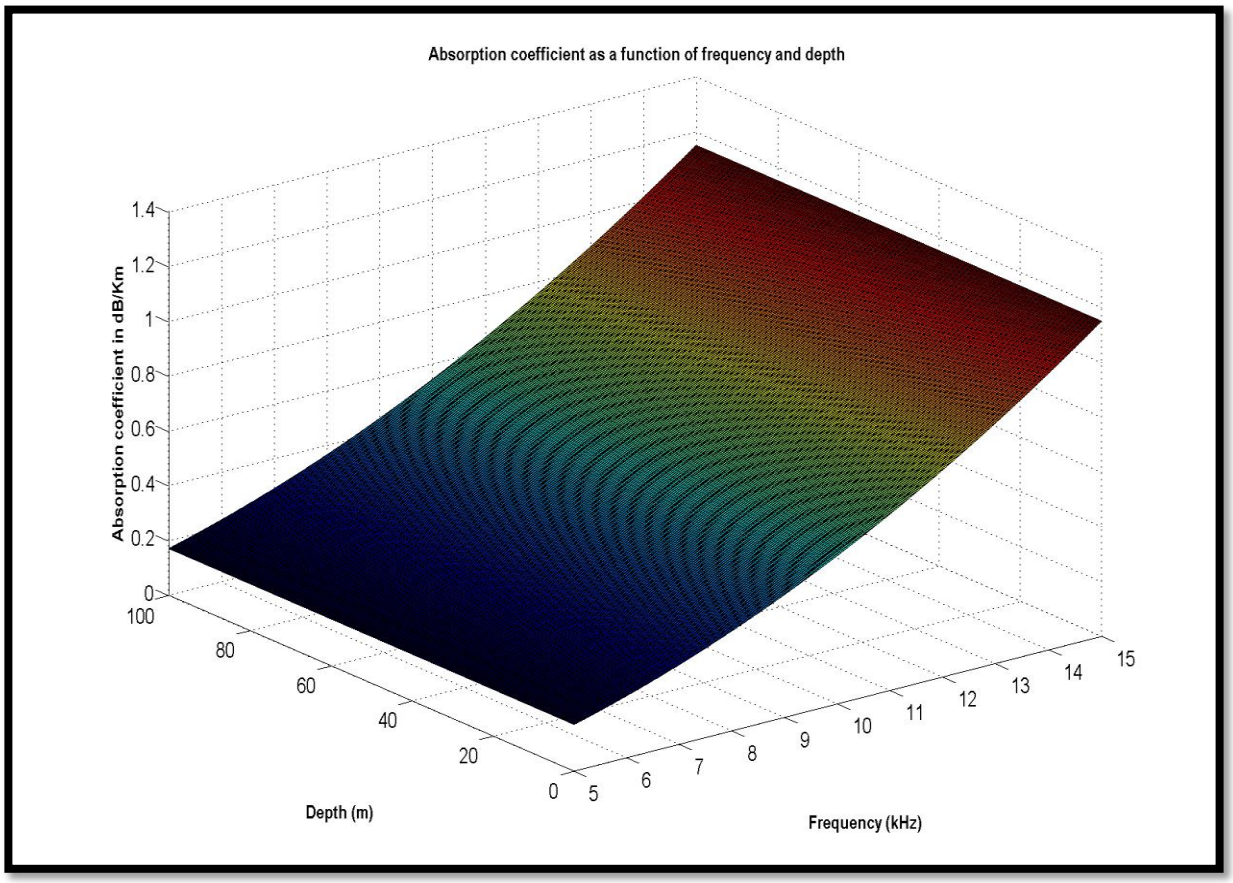

Figure 2.1: **Absorption coefficient as a function of frequency and depth.**

2.1.3 SIGNAL PROPAGATION IN SHALLOW WATER

The paths followed by a sound wave depend upon the speed structure as well as the relative location of the transmitter and the receiver [12]. In our region of interest, the shallow water of the Mississippi gulf coast, the main factors affecting the speed of the sound are temperature, pressure, depth and the salinity of the water. The empirical formula for the sound speed (in m/s) is given by [2]**:**

$$c = 1448.9 + 4.591T - 0.05304T^2 + 0.0002374T^3 + 1.340(S - 35) + 0.0163z + 1.675 \times 10^{-7} z^2 - 0.01025T(S - 35) - 7.139 \times 10^{-13} Tz^3, \quad (2.12)$$

where z is the depth in m/s, T is the temperature of the water in degree Celsius and S is the salinity in mg/l.

Equation (2.12) is valid only for:

$$0 \leq T \leq 30^0 \qquad 30 \leq S \leq 40 \ mg/l \qquad 0 \leq z \leq 8000 \ m$$

As shown in Figure 2.2, the velocity of sound underwater varies as it crosses the different layers of the sea shell. Sound magnitude slightly decreases as it passes through the surface layer, and the seasonal.

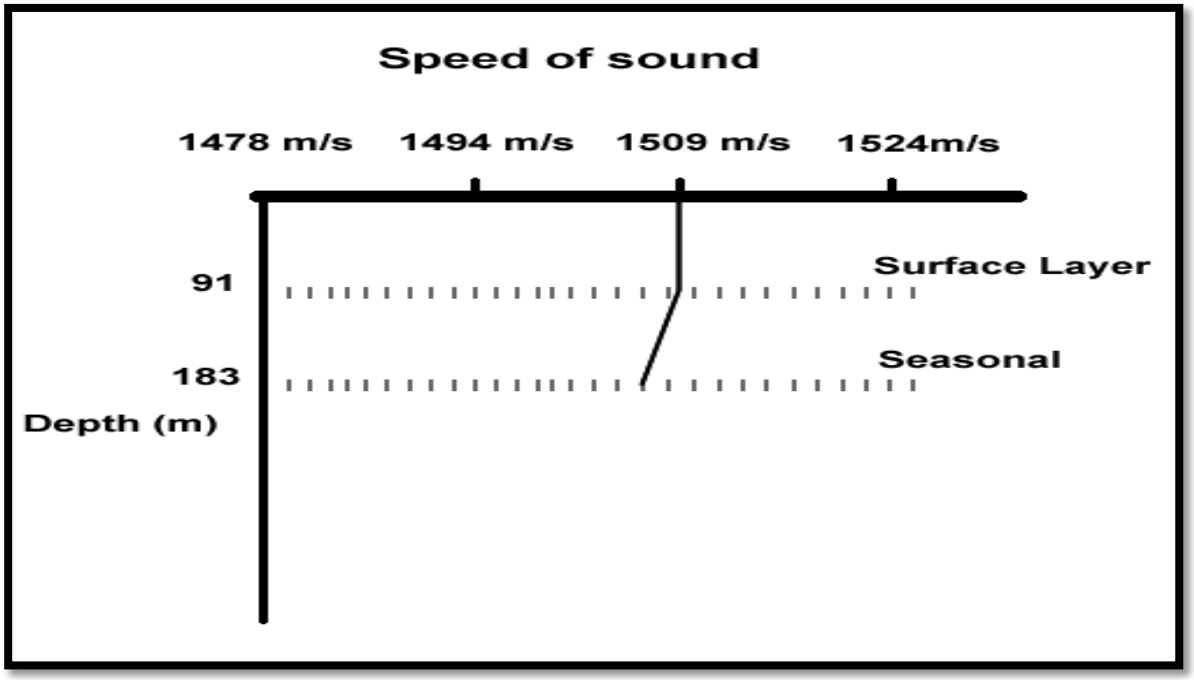

Figure 2.2: Shallow water velocity profile divided into layers [2].

The ocean is a continuum of layers. These different layers affect a sound wave in many ways. Depending on the location of the transmitter and the receiver in shallow water (see Figure 2.3), the sound wave will be subject to multipath propagation through direct path, surface reflection and bottom bounce.

In shallow water, sound is propagated mainly by continuous reflections from the surface and the bottom of the sea. The reflections at the surface have little to no loss of power while reflections at the bottoms carry the biggest attenuation depending on the type of sediments composed by the sea bottom, the angle of incidence and the sound wave frequency.

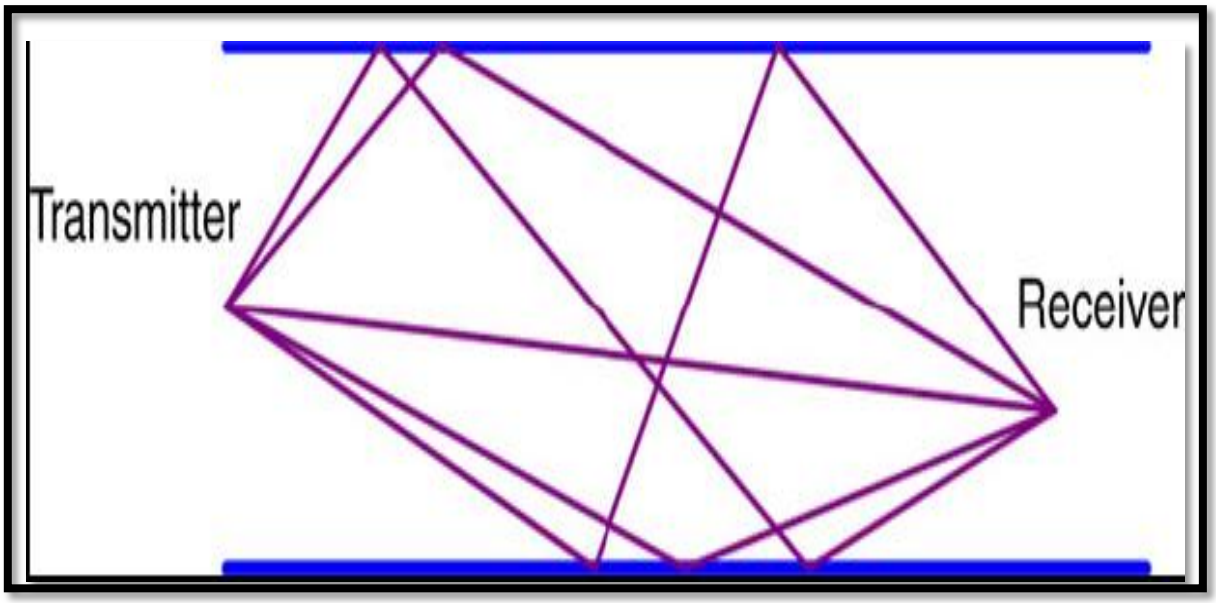

Figure 2.3: Shallow water propagation modes [2].

2.2 AMBIENT NOISE

Underwater ambient noise represents any element or sound that tends to interfere with our ability to reliably transmit data from one point to another. Multiple human and natural factors contribute to the generation of noise in shallow water. Figure 2.4 shows different sources of frequency-dependent noises in the underwater channel. Four main types of noise can be identified. They are turbulence, shipping, waves and thermal noise [2-3].

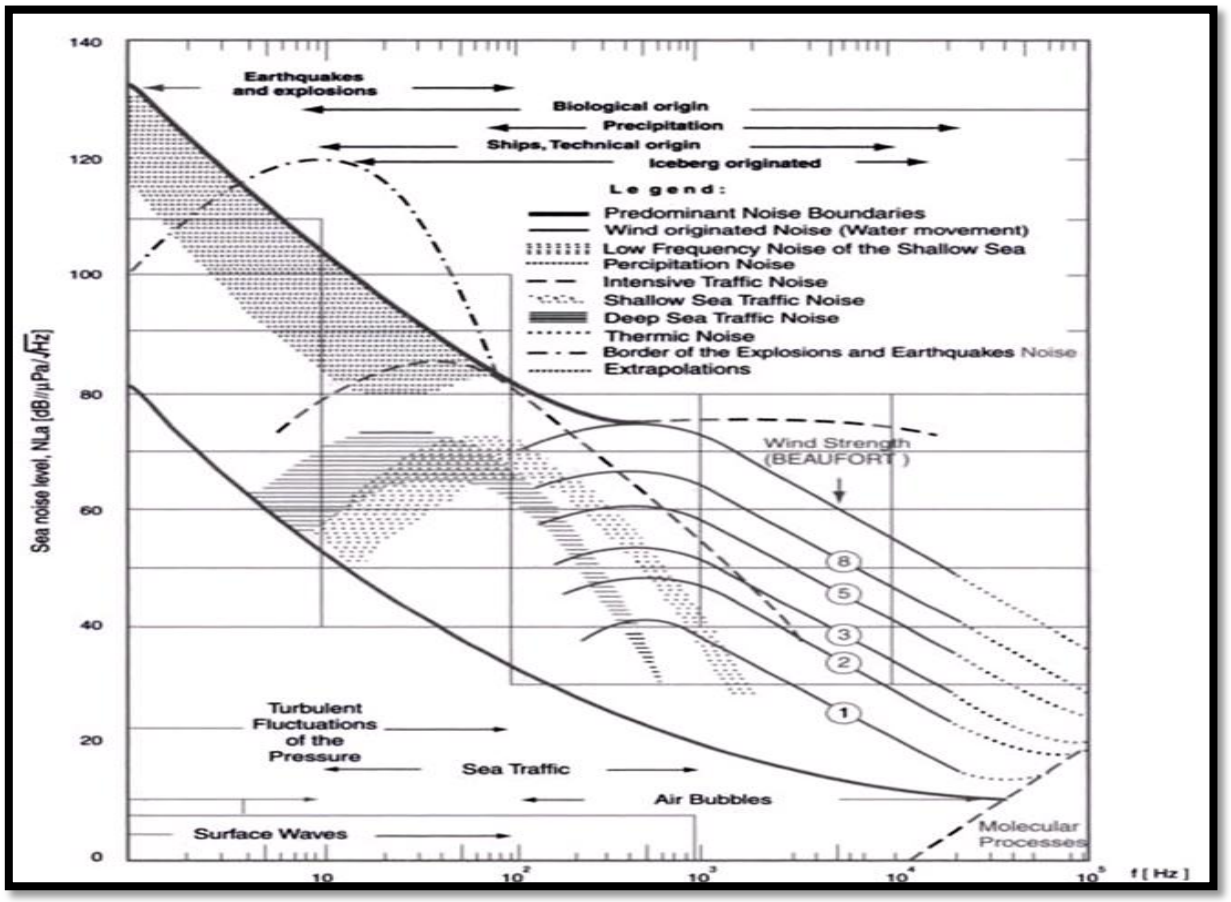

Figure 2.4: Underwater noise as a function of frequency [19].

2.2.1 TURBULENCE NOISE

Turbulence noise is generated by the movement of layers of water streaming over each other at various speeds. Turbulence is most expected at the bottom of the sea, especially in the case of shallow water were the sound wave is in contact with the seabed. The noise originating from a turbulent flow around the transmitter or receiver is more appropriately named self-induced noise rather than sea noise because noise is generated by trembling and clinking of the underwater communications devices.

The most significant acoustic effects of turbulence are caused by fluctuations of pressure inside the turbulent area. Only low frequencies, f<10 Hz are influenced by turbulence noise and therefore will not affect the system used in our research. The empirical formula for turbulence noise power spectral density (PSD), in dB re μPa per Hz, is given by [2-3]:

$$10\log\ \mathrm{N_t}(f) = 17 - 30\log\ f, \qquad (2.13)$$

where f (in kHz) is the transmitted sound signal frequency.

2.2.2 SHIPPING NOISE

Shipping noise is caused by distant shipping activity [2]. It can exhibit spatial and temporal variability. The spatial variability accounts for the distribution of shipping routes in the sea. Temporal variability is due to seasonal activities of fishing fleets. So depending on the level of boating activity in an oceanic area, shipping noise power will vary. Even if ship traffic generates sounds over a very large array of frequencies, the propagation over long distances attenuates sound at higher frequencies and only low-

frequency sound will be received. This means that shipping noise is mainly dominant in the frequency region of 10Hz to 100Hz and therefore will not affect the system used in our work. The power spectral density of shipping noise in dB r*e* µPa per Hz, is given by [2-3]:

$$10\log N_S(f) = 40 + 20(s - 0.5) + 26\log f - 60\log(f + 0.03), \qquad (2.14)$$

salinity (s) is in mg/l, and f (in kHz) is the transmitted sound signal frequency.

2.2.3 WAVES NOISE

Wave Noise can be defined as the surface motion caused by wind-driven waves. It is usually referred to as sea state noise. In fact, the sea surface waves travelling in opposite direction in the vicinity of a storm, hurricane or even windy
weather can generate a standing wave field. A standing surface wave fields produces a mean second-order pressure effect at twice the frequency of the surface waves that are not attenuated with the depth of the sea. This is the major
noise generator in the frequency region of 100 Hz to 100 kHz and therefore will be the main contributor of noise in our region of interest. The empirical formula for wave noise PSD, dB re µPa per Hz, is [2-3]:

$$10\log N_w(f) = 50 + 7.5\sqrt{w} + 20\log f - 40\log(f + 0.4), \qquad (2.15)$$

where f (kHz) is the transmitted signal frequency and w (in m/s) is the wind speed.

2.2.4 THERMAL NOISE

Thermal noise dominates in the frequency region above wind and wave generated noise, f>100 kHz and so will not affect our system. Thermal noise can simply be defined as the molecular bombardment of the receiver [20]. In fact, thermal noise underwater is generated by the same phenomenon that produces thermal noise in an electrical circuit. Because of the electro acoustic transduction process, the thermal noise pressure is proportional to frequency, and the pressure level rises approximately 6 dB per octave. Thermal noise PSD in dB re μPa per Hz, is given by [2-3]:

$$10\log \mathrm{N}_{\mathrm{th}}(f) = -15 + 20\log f, \tag{2.16}$$

where f (in kHz) is the transmitted signal frequency

3. STATISTICAL NOISE CHANNEL REPRESENTATION

Communication channel modeling is important in detection theory. Due to the randomness of the underwater medium, it is imperative to conduct a statistical approximation of the real environment of the sea. It is particularly difficult to generate an exact statistical representation of the underwater channel due to its inhomogeneity and non-stationary. It is common in the scientific and engineering world to use additive white Gaussian noise (AWGN) to represent the noise in communication channels. Although it provides researchers with fairly good approximation of the real data, it does not address specific cases of noise power distribution. In this research, we will use the power spectral density function formula given by equation (2.15) to generate a simulation model for underwater noise. Assuming a Gaussian distributed and stationary noise due to the fact that delay and phase shift are stable enough for the signal to be considered wide sense stationary. After adding the chirp signal to colored Gaussian noise, we add white noise to obtain the channel through which our data will be transmitted. The signal expression is:

$$r(t) = \alpha(t)c(b,t) + n_w(t) + n(t), \qquad (3.1)$$

where $r(t)$ represents the signal out of the underwater channel, $\alpha(t)$ is the absorption coefficient, $n(t)$ is additive white Gaussian noise, and $n_w(t)$ is colored noise computed by equation (2.15).The next paragraphs of this chapter present the noises used in our research in more details.

3.1 ADDITIVE WHITE GAUSSIAN NOISE (AWGN)

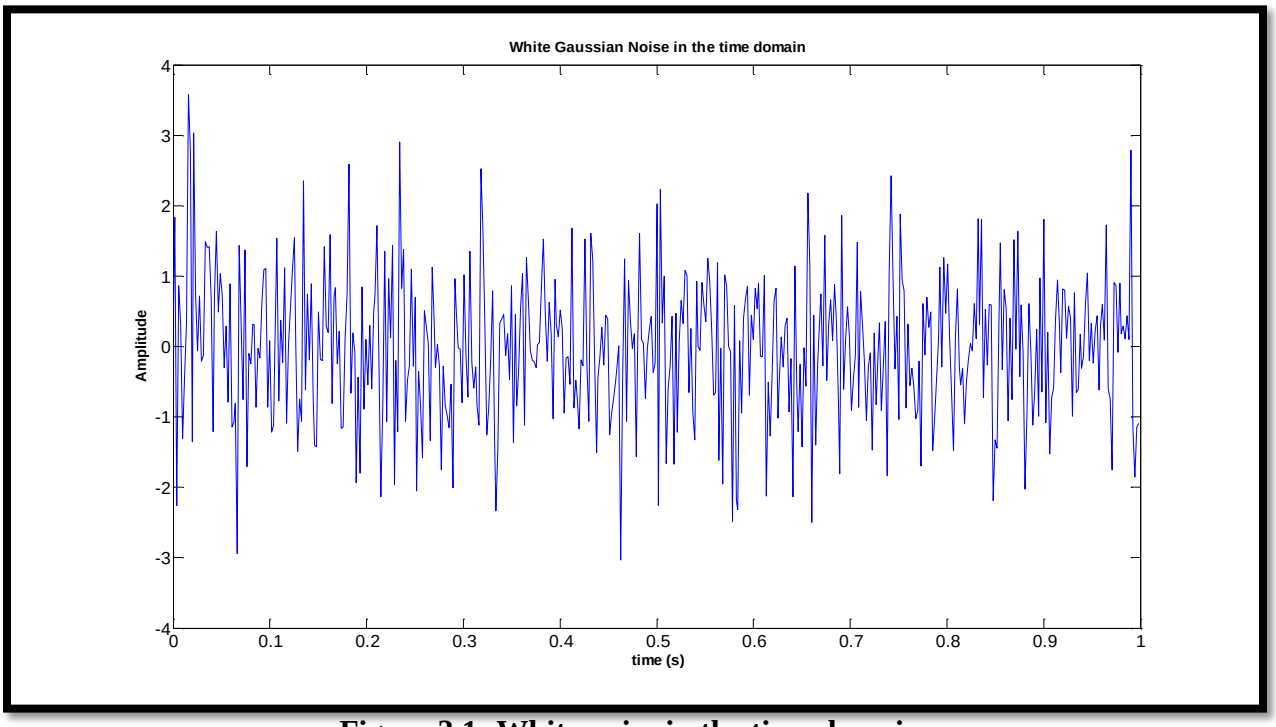

Figure 3.1: White noise in the time domain.

Figure 3.1 displays a finite length, time realization of a white noise process generated in Matlab. White noise refers to a signal whose power spectral density is flat for the entire frequency band. It is a good approximation of many real-world situations. White noise is part of the underwater channel used in this research because of our need to model the worst possible medium through which we will send data. White noise encompasses all other noise sources which are not taken into consideration in the modeling of the real underwater colored noise source because they are mathematically complex or simply unknown. White Gaussian noise has a probability density function (PDF) equals to [3]:

$$f_{\mathrm{g}}(\mathrm{n}) = \frac{1}{\sigma^2\sqrt{2\pi}}\, \mathrm{e}^{-\frac{(\mathrm{n}-\bar{\mathrm{n}})^2}{2\sigma^2}}, \qquad (3.2)$$

where σ^2 represents the variance of the noise process and $\bar{n}$ is the mean.

The signal-to-noise ratio (SNR) for white Gaussian noise is equal to [3]:

$$\mathrm{SNR_{dB}} = 10 \log\left(\frac{\mathrm{E_s}}{\mathrm{E_n}}\right), \tag{3.3}$$

E_s is the energy of one binary symbol sent and E_n stands for the double sided power of the noise.

3.2 ADDITIVE COLORED GAUSSIAN NOISE

The underwater channel in our frequencies band of interest is influenced by waves' noise. The noise has a Gaussian distribution and a power spectral density which varies with frequency. The variation of the PSD makes the noise colored. The power spectral density formula is given by equation (2.15).

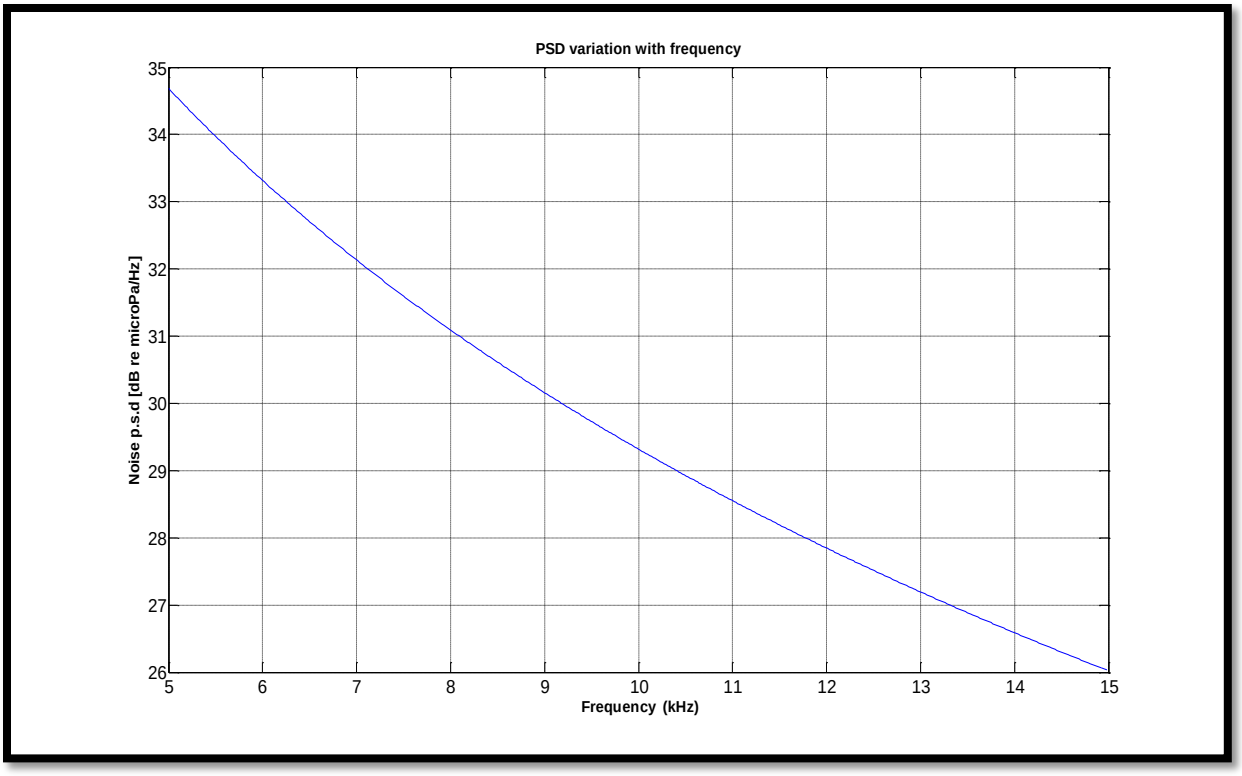

Figure 3.2 Power Spectral Density variations with Frequency

Figure 3.2 shows the wave noise power spectral density variation with frequency for a wind speed of 0 m/s. To represent our noise, we divided the PSD curve into ten equal intervals of 1000 Hz bandwidth. We proceeded this particular way because the variations of the power in these intervals of 1000 Hz were not too large. We generated white noises with each variances calculated using equation (3.4) and the corresponding frequencies intervals. We then added the noise samples together to obtain our additive colored noise shown in Figure 3.3. The expression of the double sided average power $(\mathrm{P_{av}})$ of the noise is given by [3]:

$$\mathrm{P_{av\,[}}_{f_{\min}\,,f_{\max}\mathrm{]}} = 2\int_{f_{\min}}^{f_{\max}} \mathrm{N_w}(f)\ \mathrm{d}f. \qquad (3.4)$$

The signal-to-noise ratio (SNR) of the transmitted signal is given by:

$$\mathrm{SNR_{dB}} = 10 \log\left(\frac{\mathrm{P_c}}{\mathrm{P_{av}} + \sigma^2} \right), \tag{3.5}$$

where $\mathrm{P_c}$ is the power of the chirp signal in watts, $\mathrm{P_{av}}$ is the average power of the colored Gaussian noise in watts and σ^2 is the variance of the white noise.

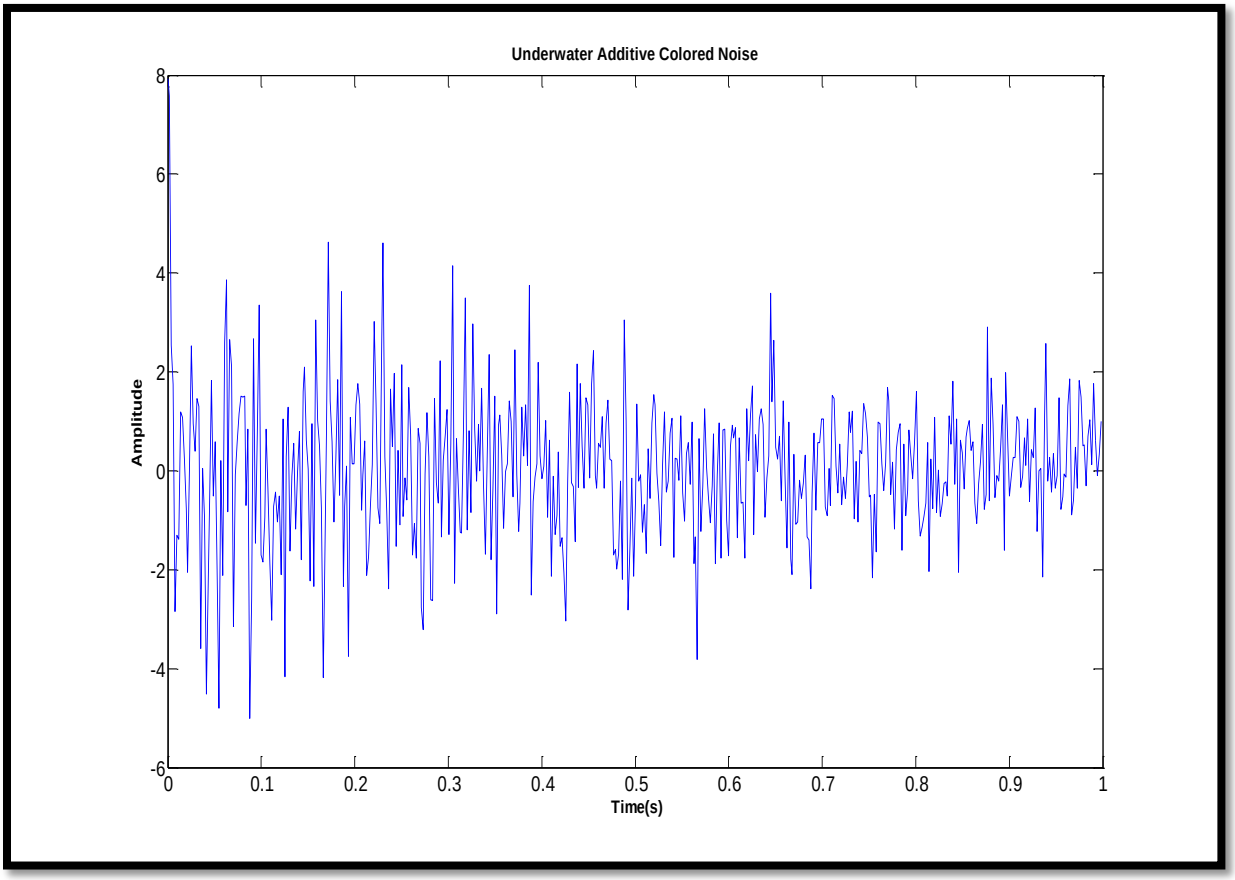

Figure 3.3: Colored noise in the time domain.

4. CHIRP- SLOPE KEYING MODULATION

Linear chirp signals generally refer to frequency modulation in radar and sonar communications [4]. Chirp modulation was first introduced in radar data transmission to enhance range resolution with pulses much longer than would ordinary be employed in high range resolution radar. Many fields such as sonar have adopted CSK due to the efficiency of the performance of related applications. Chirp modulation is classified as a spread spectrum technique due to its wide band properties [4]. Chirp signal transmission technique outperforms other modulation schemes such as amplitude-shift-keying (ASK), frequency-shift-keying (FSK), and phase-shift-keying (PSK) [1].CSK provides the information with a solid shield against multipath fading, decorrelation of impulsive type noise, jamming interference and immunity to frequency selective channels [1].

4.1 MATHEMATICAL PROPERTIES OF A LINEAR CHIRP SIGNAL

4.1.1 GENERAL EXPRESSION OF LINEAR CHIRP

In a linear chirp, the instantaneous frequency $f(t)$ varies linearly with time. Frequency can be written as [4]:

$$f(\mathrm{t}) = f_0 + \mu \mathrm{t} \ , \qquad (4.1)$$

where f_0 is the starting frequency (at time t = 0), and μ is the rate of frequency increase or decrease. μ is commonly referred to as the chirp rate. It is defined in equation (4.2)

where $f_{\max}$ and $f_{\min}$ are the maximum and minimum frequencies, respectively, of the signal for a time interval $\Delta t = t_{max} - t_{min}$.

$$\mu = \frac{f_{max} - f_{min}}{t_{max} - t_{min}}. \quad (4.2)$$

The bandwidth of the signal can be expressed as: $B = f_{\max} - f_{\min}$.

The general time-domain expression for a sinusoidal linear chirp signal may be expressed as [4]:

$$c(t) = \cos[\, 2\pi \left(f_0 + \frac{\mu}{2} t\right) t + \theta_0]. \quad (4.3)$$

Equation (4.3) becomes:

$$c(t) = \cos[\, 2\pi f_0 t + \pi \mu t^2 + \theta_0], \quad (4.4)$$

where θ_0 represents the initial phase of the signal.

4.1.2 POWER CALCULATION

A chirp signal is defined to be a power signal because it has a finite but nonzero power ($0 < P_c < \infty$) for all time, where [4]:

$$P_c = \lim_{T\to\infty} \frac{1}{T} \int_{-T/2}^{T/2} c^2(t) dt \,. \quad (4.5)$$

The power expression is then:

$$P_c = \lim_{T\to\infty} \frac{1}{T} \int_{-T/2}^{T/2} \cos^2(2\pi f_0 t \pm \pi \mu t^2) dt \,. \quad (4.6)$$

$$P_c = \frac{1}{2} + \frac{1}{2g} \left\{ \cos\left(\frac{1}{2} \pi p^2\right) . \left[C_f(p) - C_f(p+g)\right] + \sin\left(\frac{1}{2} \pi p^2\right) \left[S_f(p) - S_f(p+g)\right] \right\}, \quad (4.7)$$

where p is defined as:

$$\mathrm{p} = \frac{2f_0}{\sqrt{\mu}}\,, \tag{4.8}$$

and g is expressed as [4]:

$$\mathrm{g} = 2\mathrm{T}\sqrt{\mu}\ . \tag{4.9}$$

The Fresnel cosine and sine, respectively $\mathrm{C}_f\ (\mathrm{x})$ and $\mathrm{S}_f\ (\mathrm{x})$, are defined as:

$$\mathrm{C}_f(\mathrm{x}) = \int_0^{\mathrm{x}} \cos\left(\frac{1}{2}\ \pi \mathrm{t}^2\right)\ \mathrm{dt}\ , \tag{4.10}$$

$$\mathrm{S}_f(\mathrm{x}) = \int_0^{\mathrm{x}} \sin\left(\frac{1}{2}\ \pi \mathrm{t}^2\right)\ \mathrm{dt}\ . \tag{4.11}$$

Assuming that the arguments of the Fresnel sine and cosine are large in the expression of the chirp power, $\mathrm{C}_f(\mathrm{x})$ and $\mathrm{S}_f(\mathrm{x})$ approach $\frac{1}{2}$. The power of the chirp is:

$$\mathrm{P_c} = \frac{1}{2} + l\ , \tag{4.12}$$

with $l \ll \frac{1}{2}$.

4.2 UP-CHIRP

A linear up chirp is a signal with an increasing frequency vs time. This signal is composed of a wide or narrow band of frequency that gradually increases [4]. The signal changes in time from a low tone to a high one. In our work, the minimum carrier frequency is 5000 Hz while the maximum frequency is 15000 Hz. The spectrogram of a linear up-chirp as shown in Figure 4.1 demonstrates the positive linear rate of change in frequency as a function of time from 5 kHz to 15 kHz.

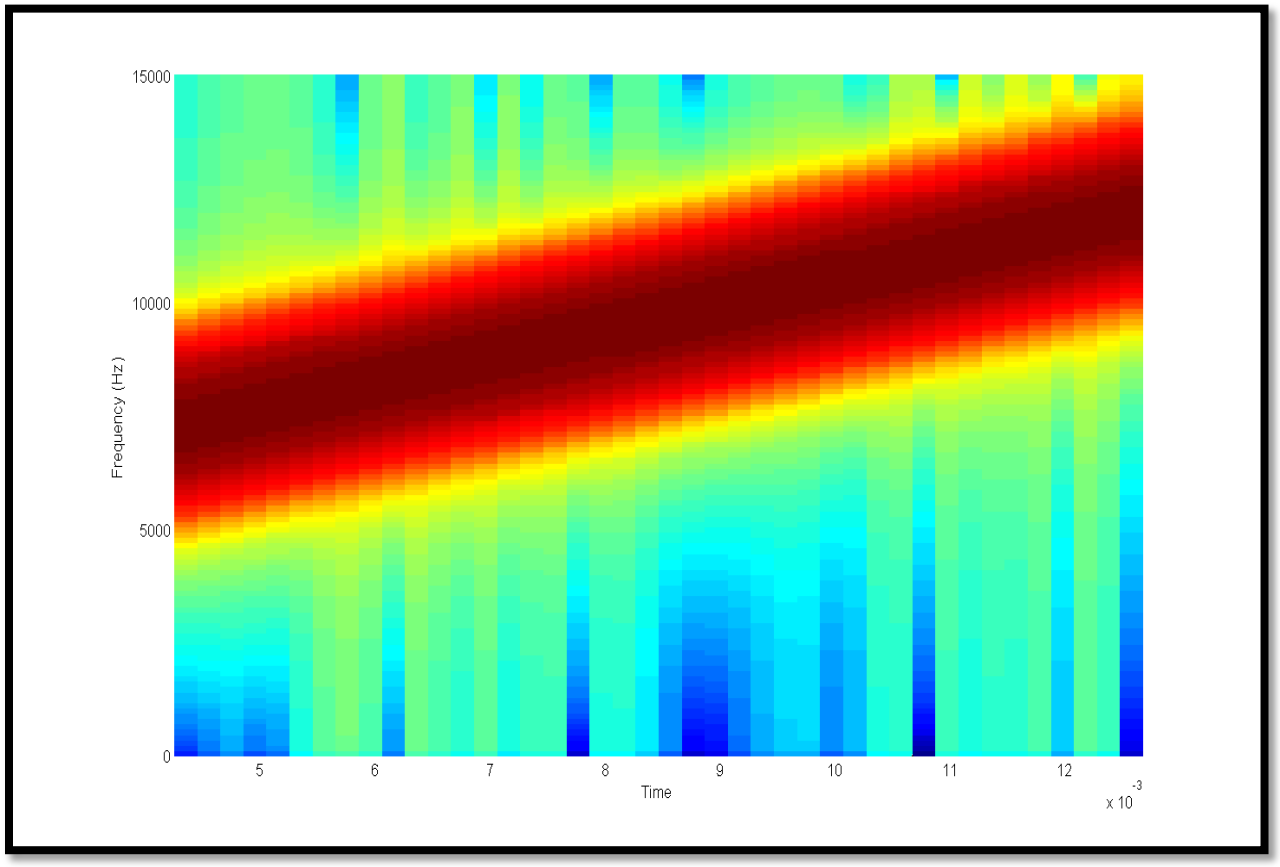

Figure 4.1: Linear Up-Chirp spectrogram.

4.3 DOWN-CHIRP

A down chirp is a linear chirp signal with a decreasing frequency vs time. As opposed to the up chirp, the signal changes from a high pitch to a low pitch. The reference starting frequency is higher than the ending frequency. In our work, the down chirp signal starts at 15 kHz and decreases to 5 kHz. The spectrogram of the chip signal in Figure 4.2 demonstrates the negative linear rate of change in frequency as a function of time from 15 kHz to 5 kHz.

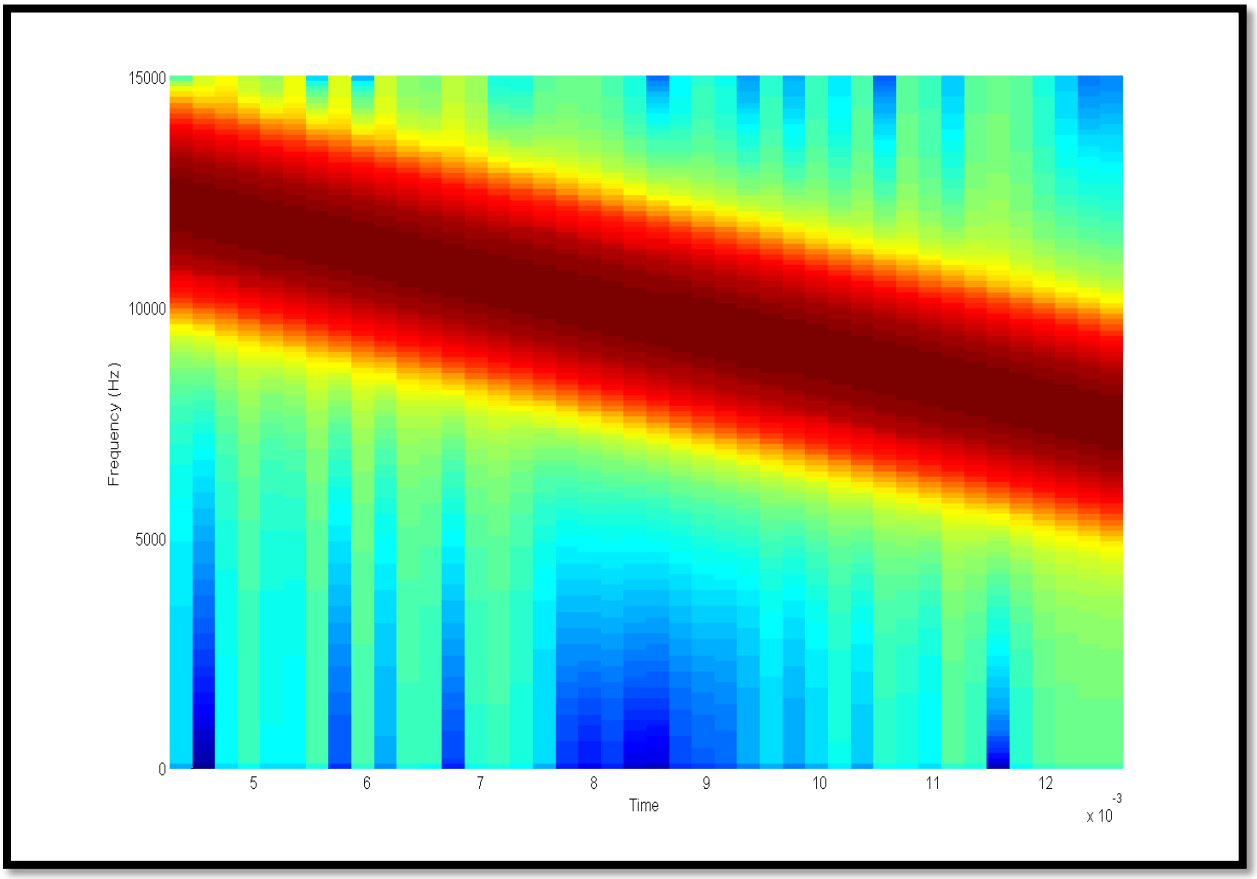

Figure 4.2: Linear Down-Chirp spectrogram.

4.5 CHIRP-SLOPE KEYING MODULATION

Basic operations of digital data transmission and reception are explained using a block diagram as shown in Figure 4.3. Communication in the air and underwater follows the same general concept. However, a slight difference resides in the design of transmitters and receivers used in either medium. Chirp-slope keying (CSK) is a modulation technique that can be used in underwater digital data communication. In CSK, binary numbers are used to modulate chirp signals. Binary designates a coding scheme which used two numbers, each number referring to a bit in digital systems. In our research, we use '0' and '1'. A general digital communication model, which is valid for data processing in any transmission channel, is divided into three main parts: a digital transmitter, a channel and a digital receiver.

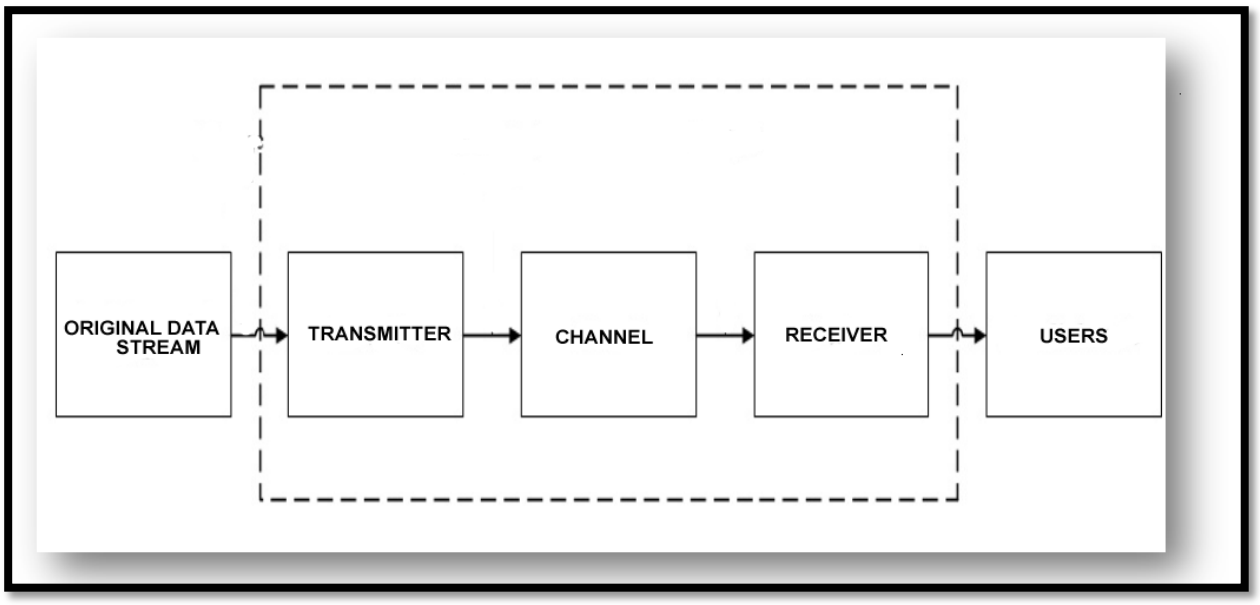

Figure 4.3: General modulation block diagram.

In Figure 4.3, a stream of digital information is sent by a source, the transmitter transforms the binary digital signal into a waveform which will then be sent through the transmission channel. The receiver converts the signal back to a binary signal and hopefully gives a satisfying and reliable estimate of the original set of data sent.

The general concept of digital data transmission is applied in our research using a linear chirp signal modulated by the bits to be transmitted. At the transmitter, each bit is mapped with its equivalent chirp signal. The signal generated can be expressed as: $c(b,t)$ .The chirp is both a function of the binary digit value and time. Including these two variables in the general equation of a chirp signal, equation (4.4) becomes:

$$c(b,t) = \cos[\,2\pi f_0 t + \pi\,\mu(2b-1)t^2 + \theta_0]\ , \qquad (4.13)$$

with θ_0 equals to zero.

The signal coming out of the underwater channel is given by equation (3.1).The received signal is demodulated by passing it through a correlator receiver and converting it back to a digital stream of data. More details about CSK modulation are given in Chapter 5 which deals with the description of the system.

5. SYSTEM DESCRIPTION

The detailed system is divided into three main parts: the transmitter, the channel and the receiver. Figure 5.1 describes the system used in our simulations.

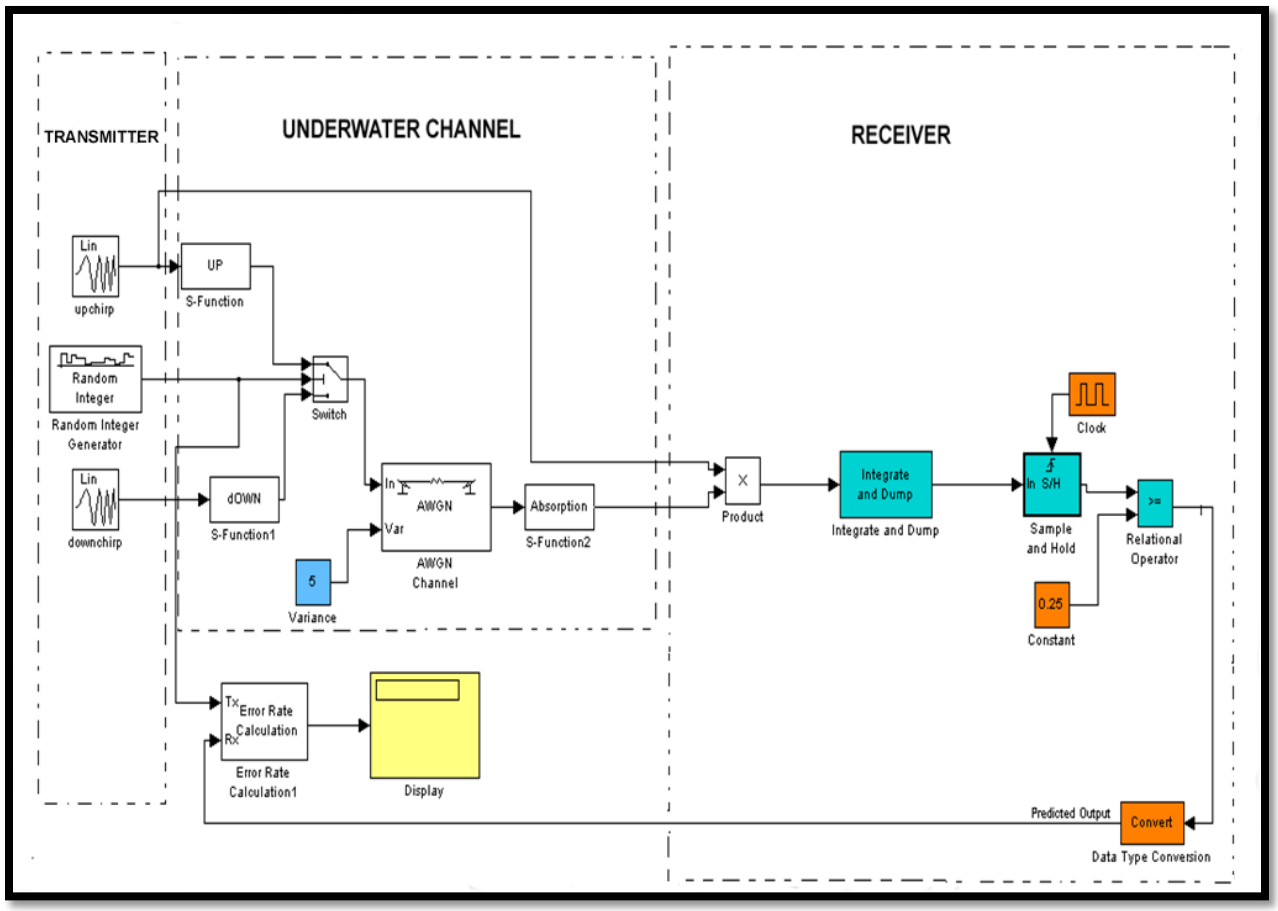

Figure 5.1: CSK communication system Simulink model

5.1 TRANSMITTER BLOCK

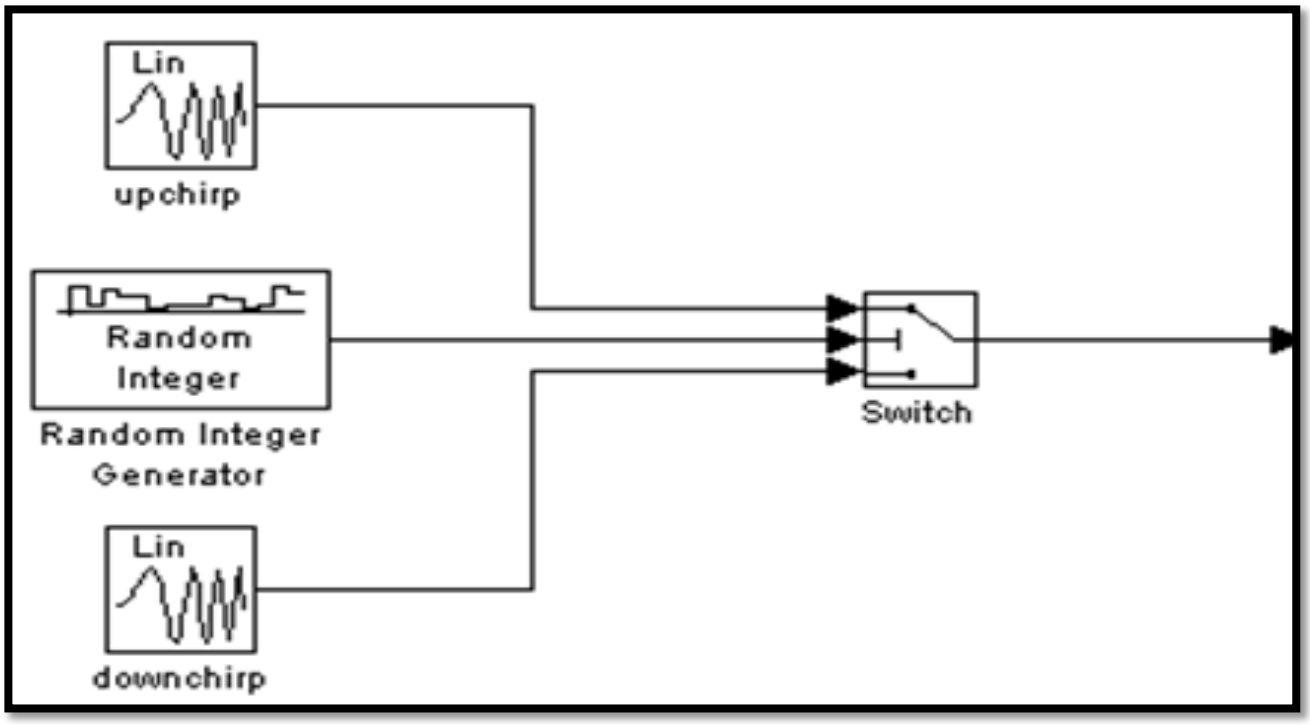

Figure 5.2: Transmitter block's Simulink model.

The transmitter, shown in Figure 5.2, encompasses the digital data modulator and the chirp signal modulated by the random sequence of binary digits. The Random Integer generator block generates uniformly distributed random binary integers either 0 or 1. The up-chirp signal block generates a cosine chirp whose frequency increases at a linear rate μ defined by equation (4.2). The down- chirp on the bottom side generates a sine chirp whose frequency decreases at the same linear rate as the up-chirp. The up-chirp represents binary data of value equals 1 while the down chirp represents data of '0' value. We introduce a switch block which plays a multiplexing role. The switch passes through the first or the third input based on the value of the second input. If the

second input value is 1, the switch passes the up-chirp while blocking the down-chirp. The reverse operation happens when the second input has a zero value. In Figure 5.3, there are two oscilloscope displays. The first one represents the binary stream of data modulating our chirp signal while the second display represents the modulated chirp signal sent through the communication channel.

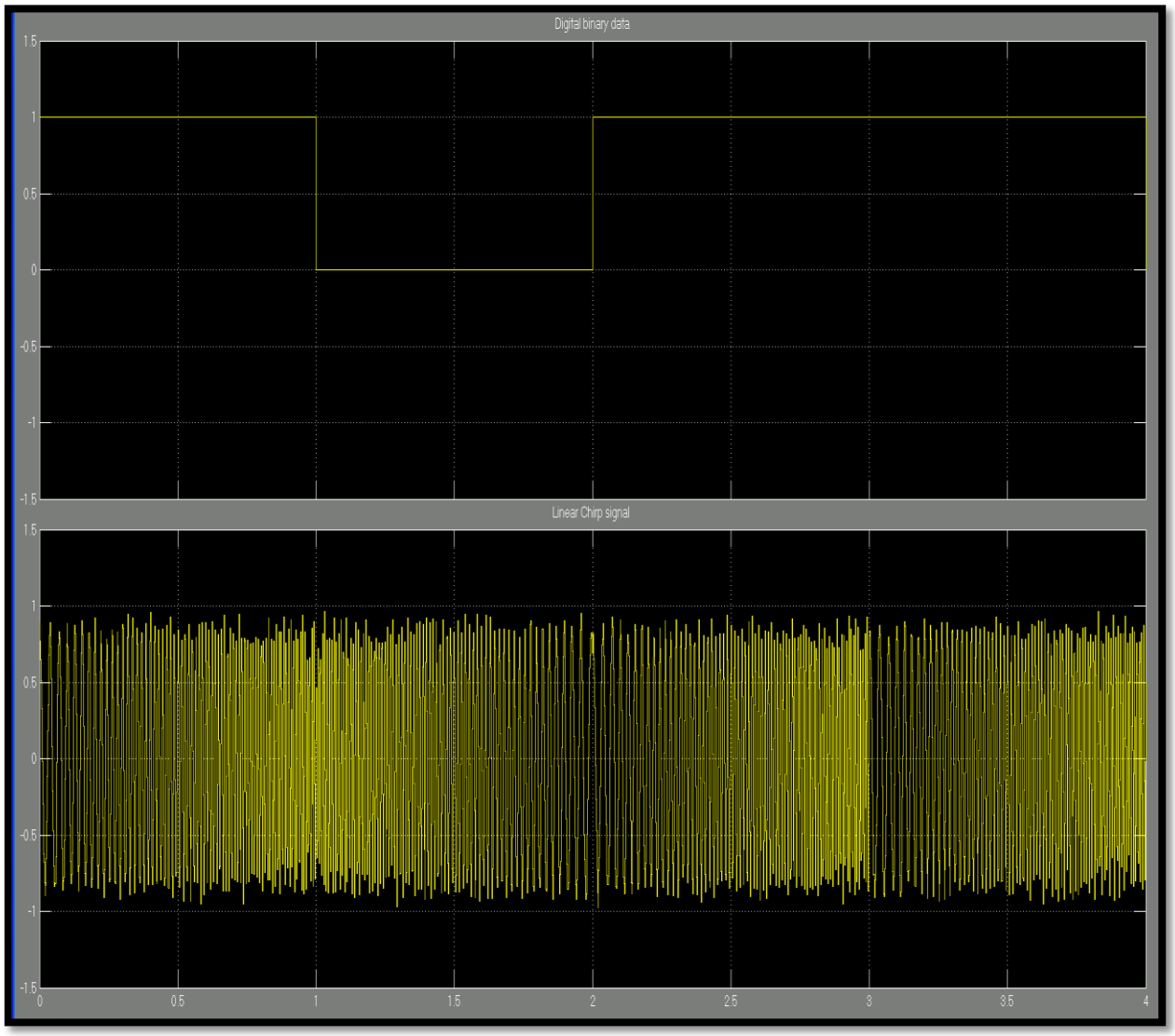

Figure 5.3: Output of transmitter block.

5.2 CHANNEL BLOCK

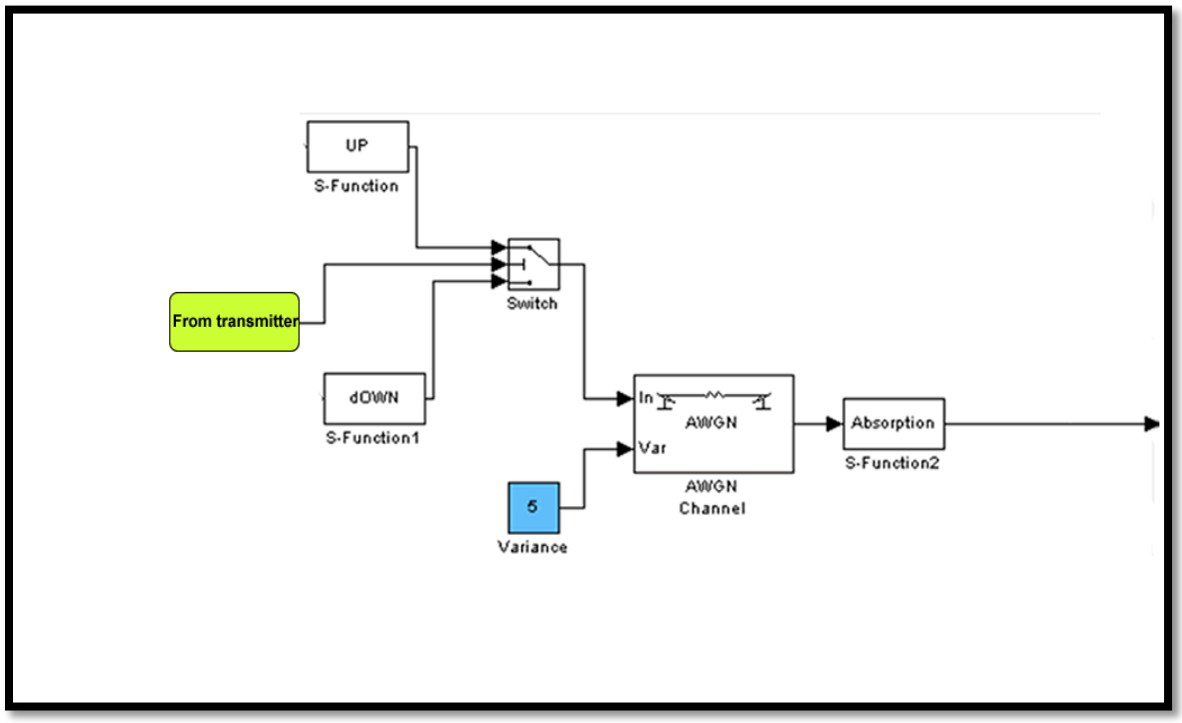

Figure 5.4: Channel block's Simulink model.

Our area of interest is the shallow waters of the Mississippi Gulf coast. Using equations (2.3), we calculate the values of the absorption coefficient (see appendix) for different frequencies and the variances needed to generate our wave noise. In Simulink, there aren't blocks capable of accurately representing the colored Gaussian noise, and the absorption coefficient used in our research. To remedy this problem, we used s-functions to program (see appendices F and G), and incorporated them in our simulation model.

The AWGN block adds white Gaussian noise to the input signal. The white noise variance can be adjusted using the variance block which computes the unbiased variance of the noise. Figure 5.5 shows the signal received by the receiver.

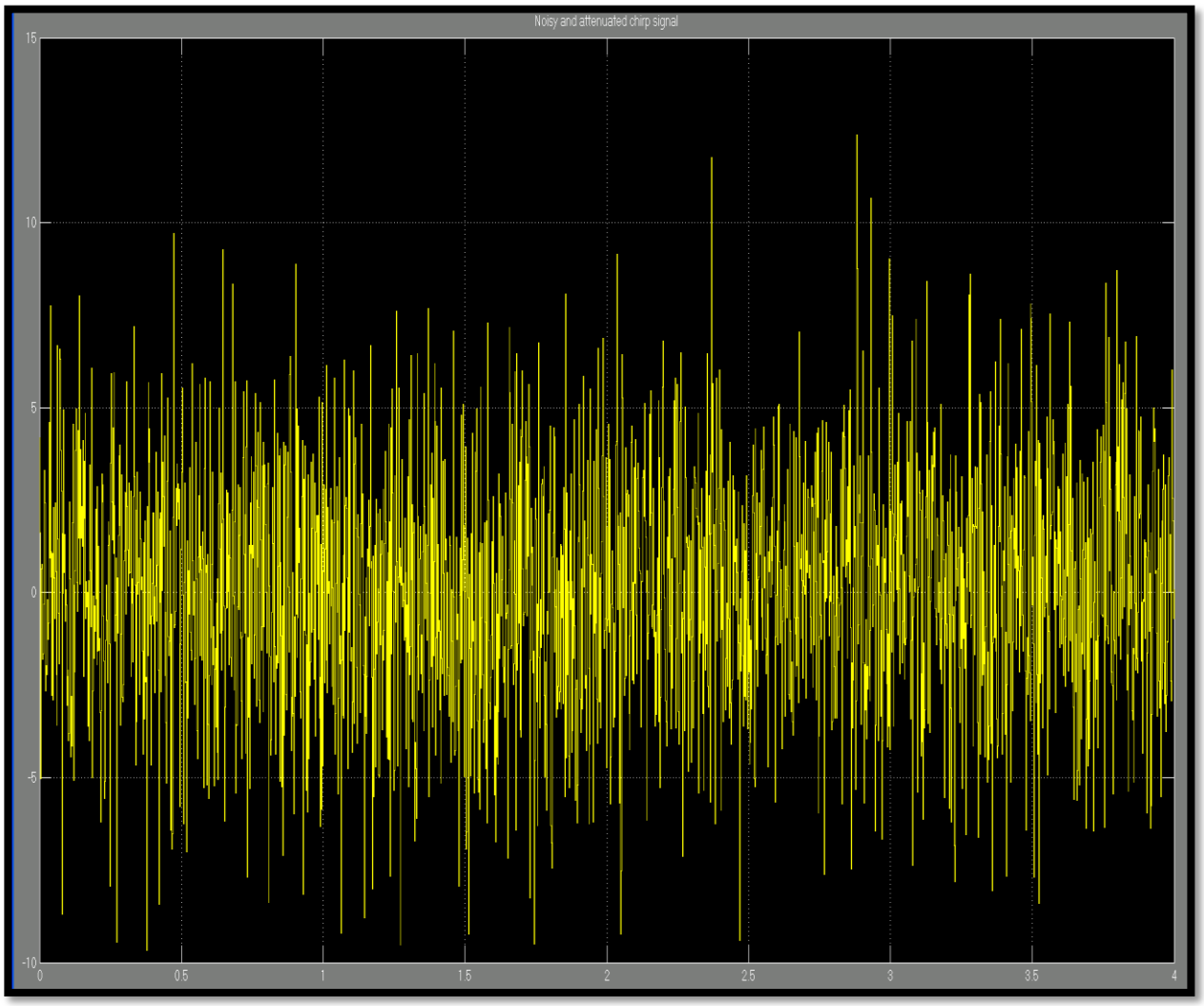

Figure 5.5: Output of Channel block.

5.3 THE RECEIVER BLOCK

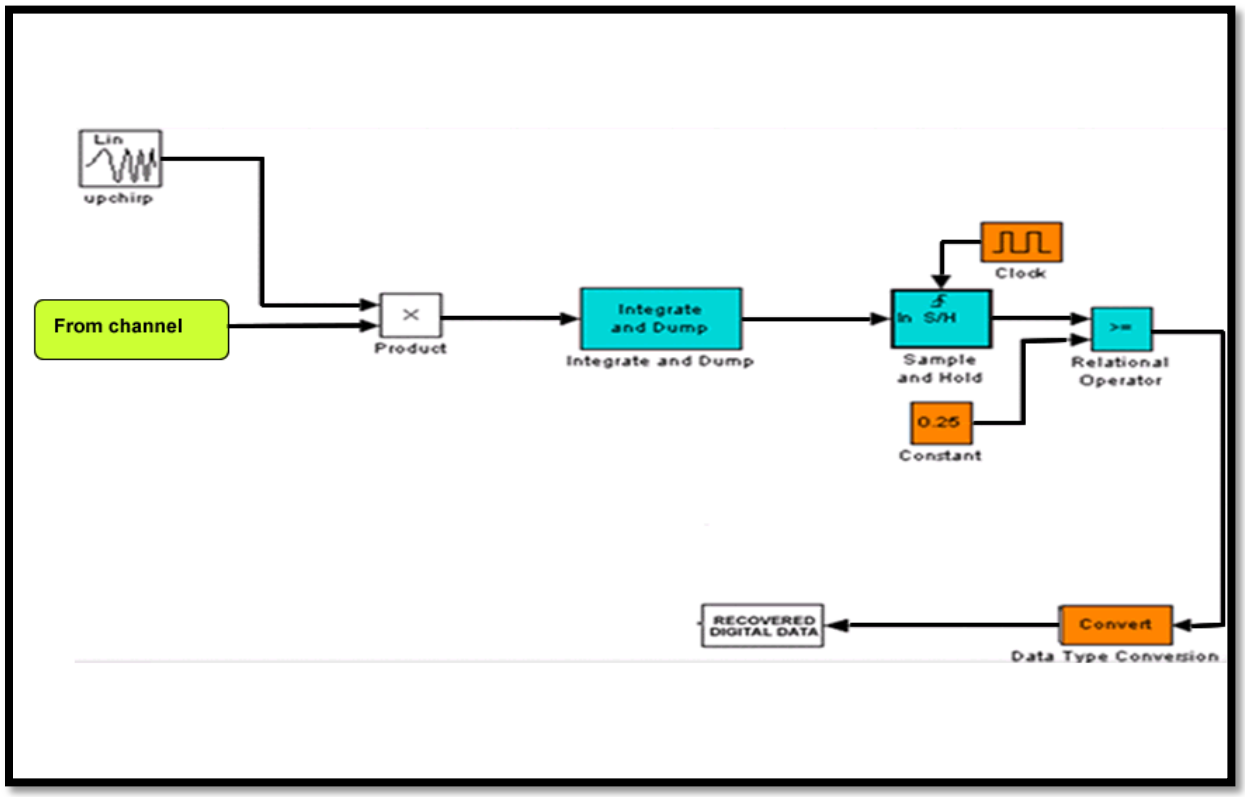

Figure 5.6: Receiver block's Simulink model.

The receiver reproduces out of the channel output, as accurately as possible, the binary data sequence sent. The main component of the receiver is the correlator receiver. A correlator is a linear filter designed to provide the maximum signal-to-noise power ratio at its output for a given transmitted signal.

The integrate and dump block in figure 5.6, is the component of the correlator to creates a cumulative sum $z(T)$, of the discrete-time input signal while resetting the sum to zero every period of the chirp signal. The integrate and dump block acts as a low pass filter.

The sample and hold block acquires the sum $z(T)$ from the previous block and hold it until it receives a trigger signal. This signal comes from the clock which is set to the

period of a symbol (1 second in our work). In other words, the block releases the data to be processed by the next entity as soon as it receives a clock pulse.

After the data are released, they are compared to a threshold γ which is set to half of the maximum sum calculated by the integrate and dump section of the system. In our research, the maximum sum calculated is approximately equal to 0.5, so we set $\gamma = 0.25$. When $\mathrm{z(T)} > \gamma$, the relational operator in Figure 5.6 outputs a boolean "true". When $\mathrm{z(T)} < \gamma$, it outputs a boolean "false". The convert block transforms "true" into a '1' binary symbol, and "false" into a '0' binary symbol. Figure 5.7 represents the different stages of the entire correlator receiver process. There are 5 oscilloscope displays for each step of the correlator receiver. The first one from the top, represents the product of the received signal, of (3.1), by a replica of the transmitted signal. The second display shows the output of the integrate and dump block, while the third one represents the output of the sample and hold block. The relational operator and the data type conversion blocks' output are shown in display 4 and 5.

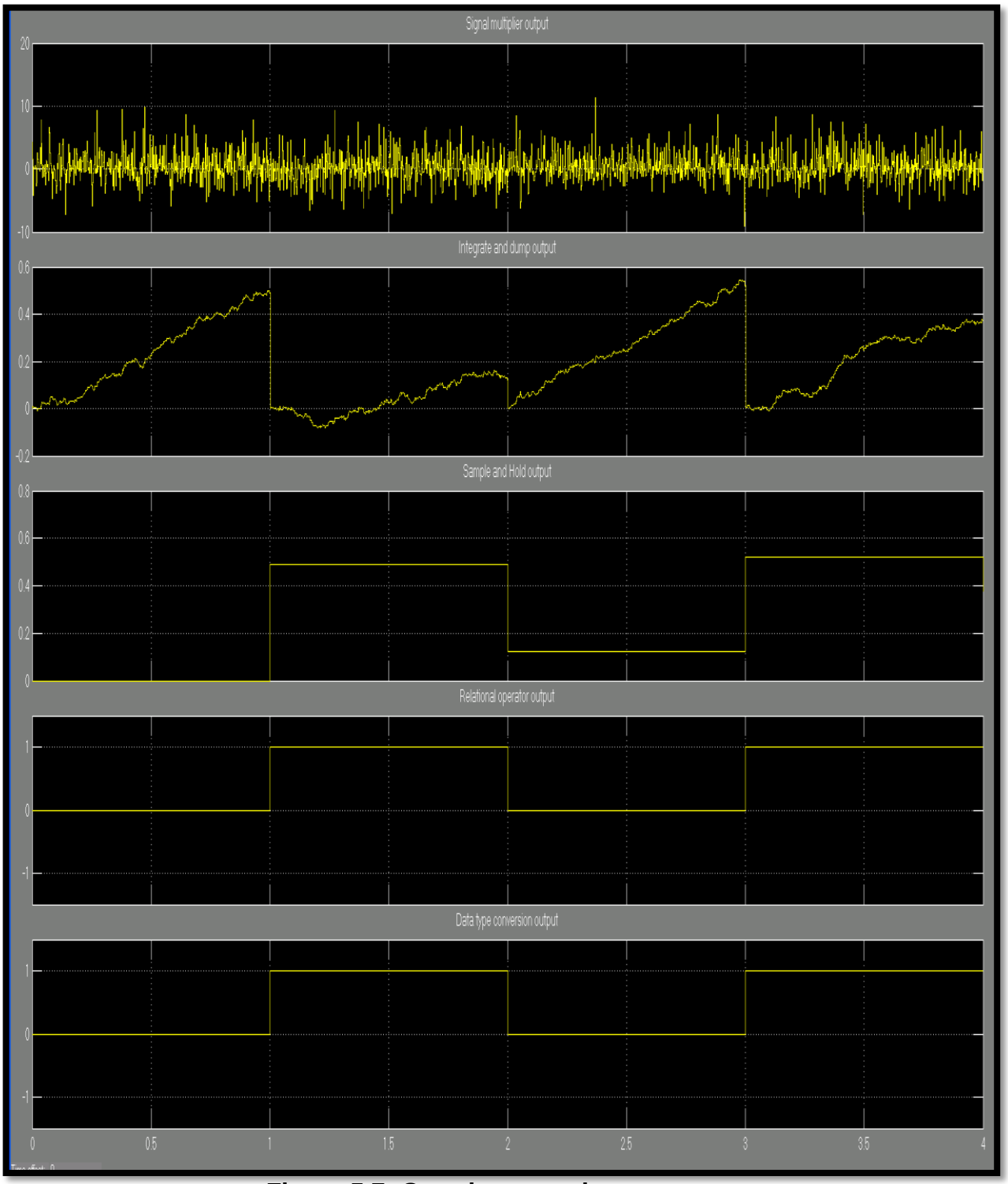

Figure 5.7: Correlator receiver outputs.

6. SIMULATION RESULTS AND DISCUSSION

This chapter presents the models used for our simulations and the results. The chirp-slope keying modulation is simulated for several wind speeds. We will give an overview of how the simulations are performed and then we will present the results of CSK with additive white Gaussian noise and colored noise. The simulations are run with four wind speeds. We decided to use wind speed values ranging from 0 m/s to 7 m/s because they are closer to the real ocean's environment. For our chirp signal, the maximum frequency is $f_{\max} = 15000\ \text{kHz}$, therefore the Nyquist frequency is:

$f_s = 2\, f_{\max} = 30000\ \text{Hz}$, thus the minimum sampling time is:

$\text{T}_\text{s} \geq \frac{1}{30000} = 3.33.10^{-5}\text{s}$.This sampling time does not offer time efficiency in the simulations. Thus, before running our simulations, we had to translate our frequency range from [5 kHz – 15 kHz] to [25 kHz – 125 kHz] to avoid interminable computational operations. The parameters used in our simulations are:

Minimum frequency: $f_{\min} = 25\ \text{Hz}$

Maximum Frequency: $f_{\max} = 125\ \text{Hz}$

Slope / Chirp rate: $\mu = 100\ \text{Hz/T}$

Sampling rate: f_s= 1/512 samples per period

Symbol duration T = 1sec

In Simulink, we run the CSK model by modulating chirps with multiple binary digits and compute the probability of error for each SNR value selected. Depending on how strong the noise corrupting the signal is, it takes different number of sent symbols to reach the 10 bits errors at which we stop the simulation. Some probabilities of errors for

high SNR were obtained after weeks of uninterrupted simulations. For each wind speed, we selected the white noise variance σ^2 between 100 and 0. The variance of the channel colored noise stays fixed with a particular wind speed. It only changes when the wind speed changes.

The probability of errors is: $\left(\mathrm{P_e} = \frac{\text{Errors}}{\text{Number of bits sent}} \right)$. (6.1)

6.1 WIND SPEED = 0 m/s

For $w = 0\ \mathrm{m/s}$, we have a relatively calm ocean, although there is a slight presence of noise, the average power is not very high. Equation (3.5) becomes:

$$10\log N_w(f) = 50 + 20\log f - 40\log(f + 0.4), \quad (6.2)$$

with f in kHz.

In figure 6.1, for an additive white noise variance of 1, we sent $5.848\text{x}10^5$ bits to reach our desired 10 errors. The probability of error P_e is $1.71\text{x}10^{-5}$. We were unable to reach a probability of error of 10^{-6} for this wind speed because the simulation was running for a very long time and showed no sign of stopping soon. Figure 6.2 represents the probability of error ($\mathrm{P_e}$) for different SNR values.

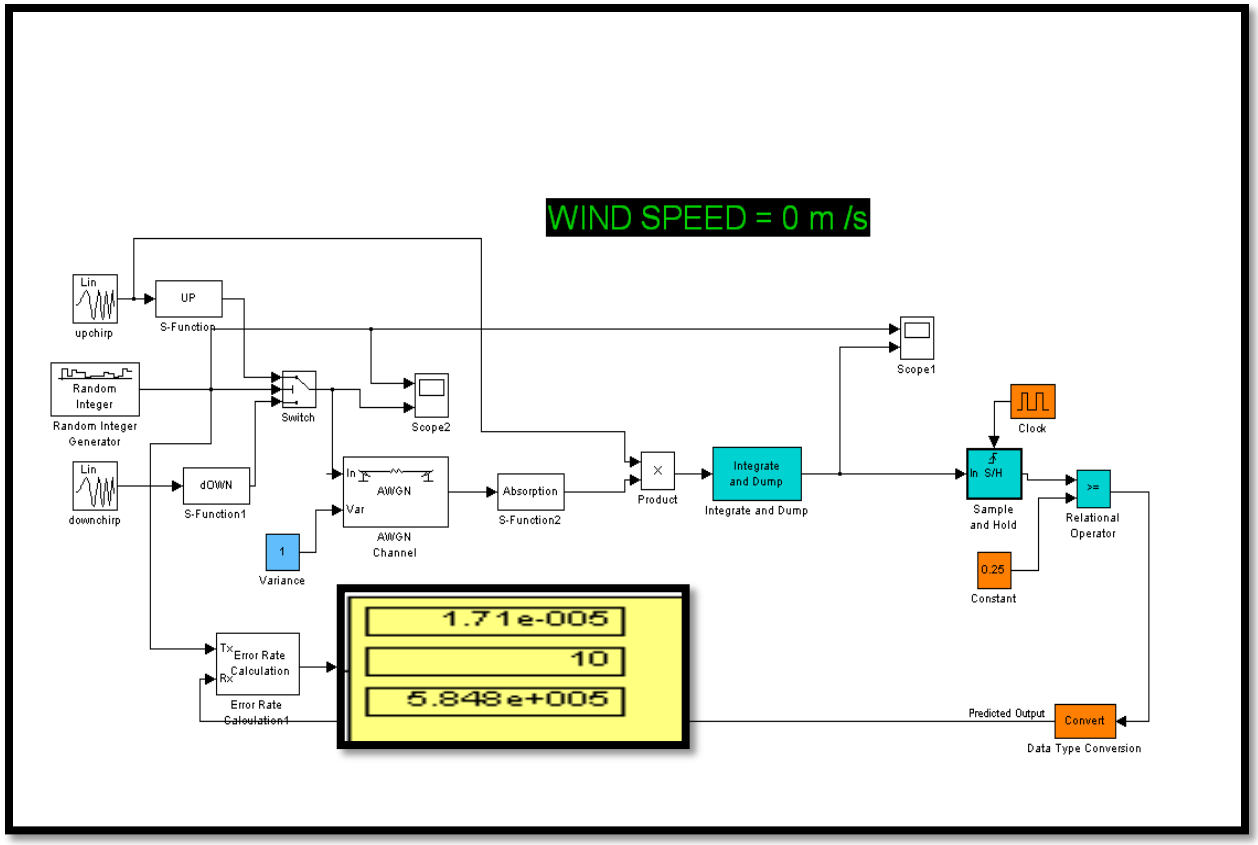

Figure 6.1: CSK for wind speed = 0 m/s and AWGN variance = 1.

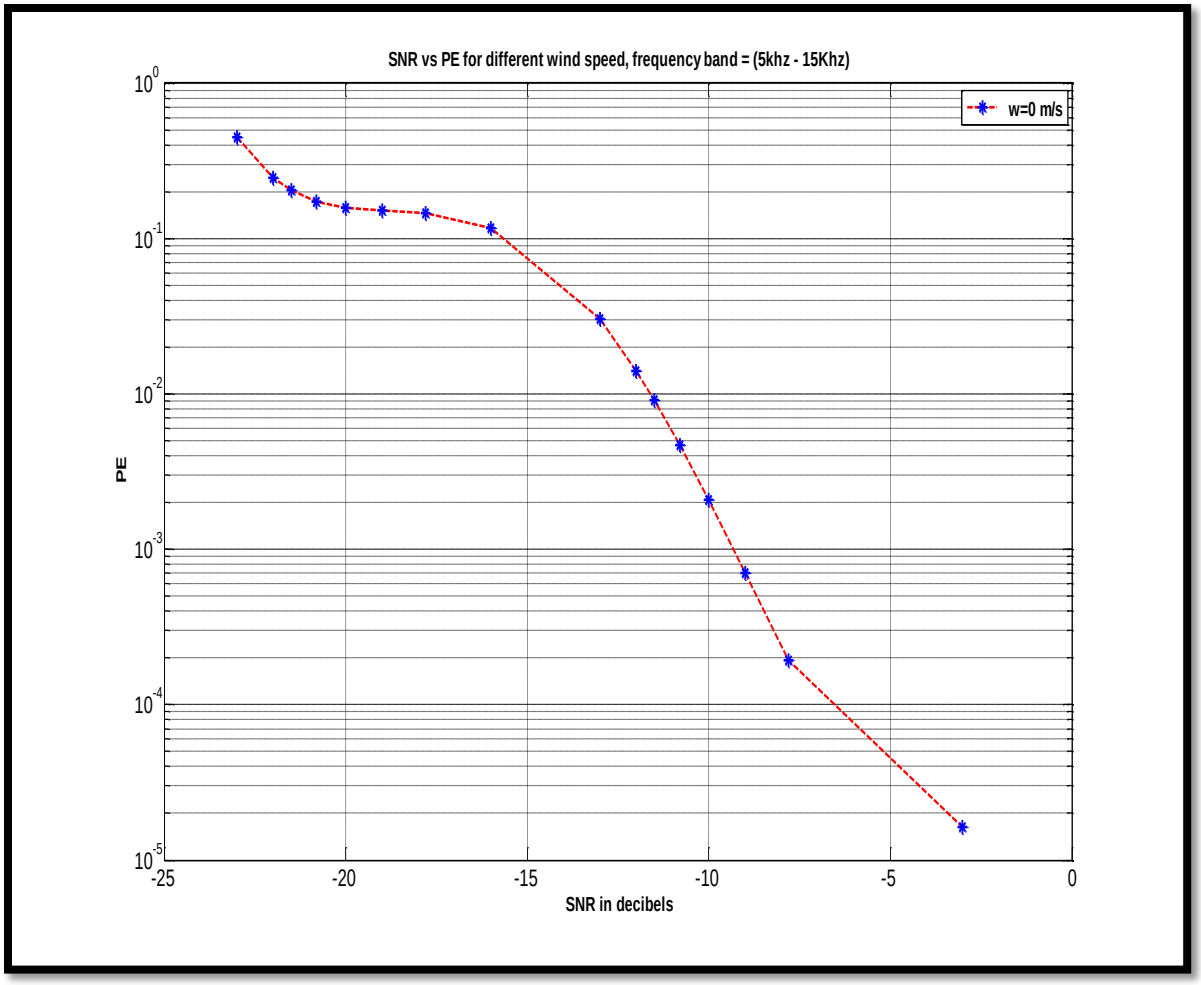

Figure 6.2: Probability of error of CSK for w = 0 m/s.

6.2 WIND SPEED = 2 m/s

A wind speed of $2\ \mathrm{m/s}$ produces a mild activity of waves in the ocean. The average power of the channel noise is slightly greater than the previous model simulated. Equation (2.5) becomes:

$$10\log \mathrm{N_w}(f) = 50 + 7.5\sqrt{2} + 20\log f - 40\log(f + 0.4)\ . \qquad (6.3)$$

In Figure 6.3, for an additive white noise variance of 0, we sent $2.666\mathrm{x}10^{6}$ bits to reach our desired 10 errors. The probability of error P_e is $3.751\mathrm{x}10^{-6}$.To obtain a probability of error of 10^{-6}, we used a sampling rate f'_s= 1/256 samples per period, higher than f_s. Our simulation was faster but there was an aliasing problem when we tried to incorporate the data in Figure 6.4 ($\mathrm{P_e}$ vs SNR plot).

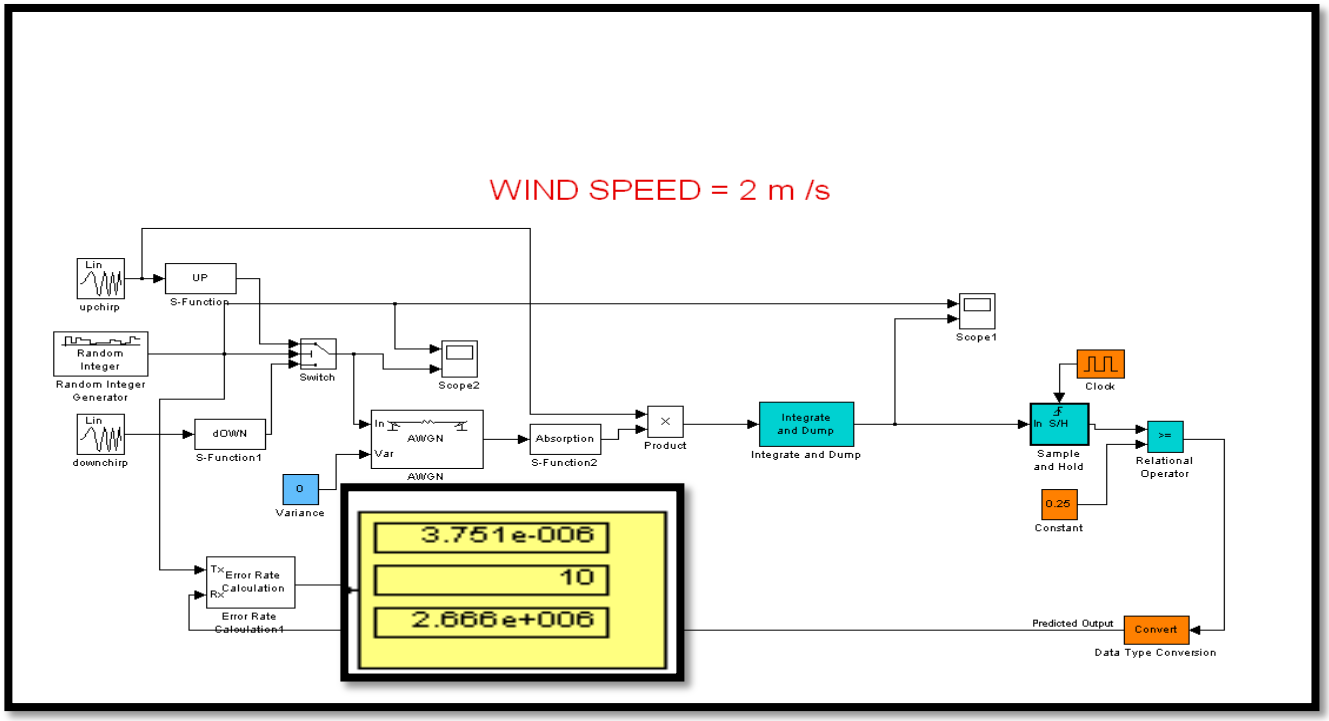

Figure 6.3: CSK for wind speed = 2 m/s and AWGN variance = 0.

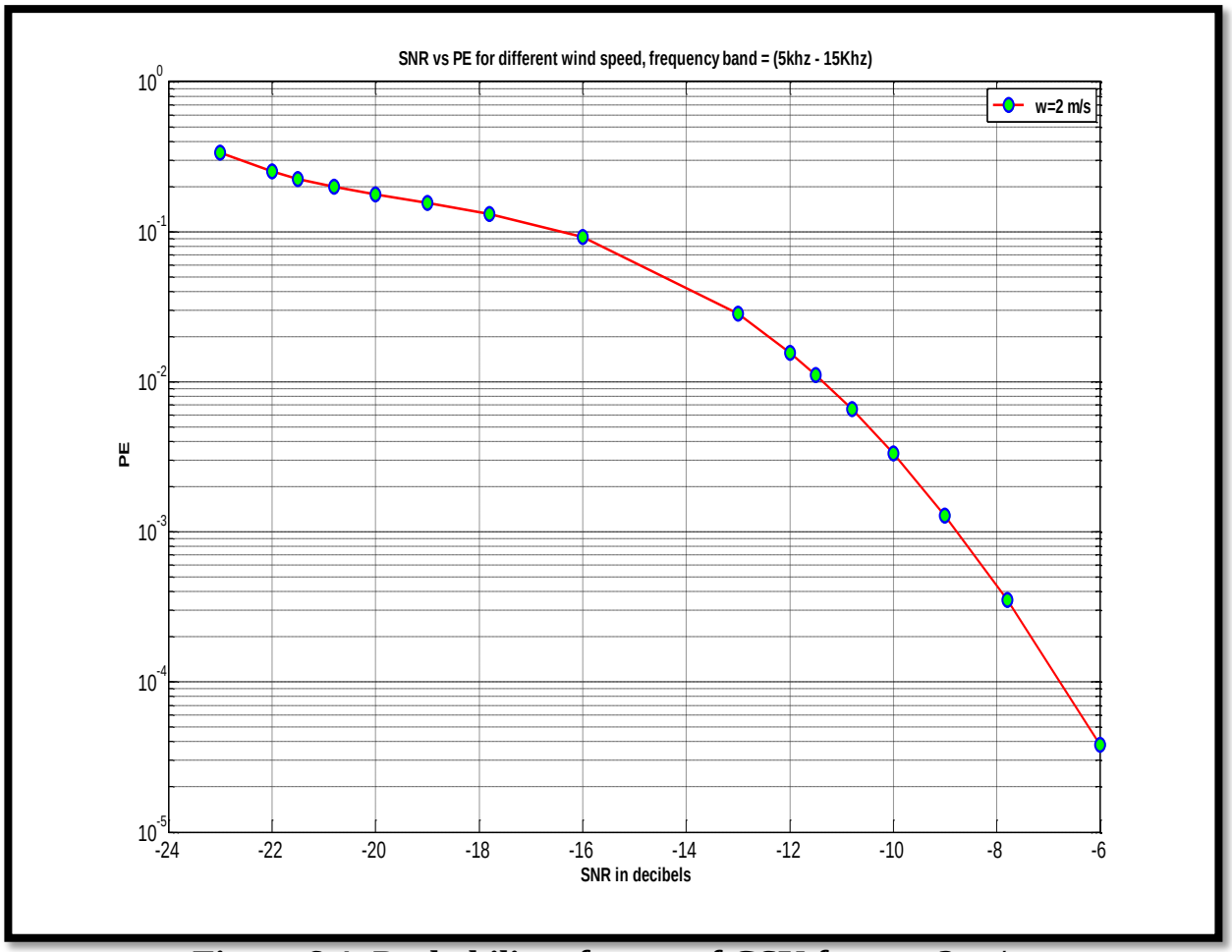

Figure 6.4: Probability of error of CSK for w = 2 m/s.

6.4 WIND SPEED =5 m/s

At 5 m/s or 18 km/hr, the ocean is very agitated. There is a lot of waves activity and the average power of the noise is large. Equation (3.5) becomes:

$$10\log N_w(f) = 50 + 7.5\sqrt{5} + 20\log f - 40\log(f + 0.4). \qquad (6.4)$$

Figure 6.5 represents the probability of error (P_e) vs SNR.

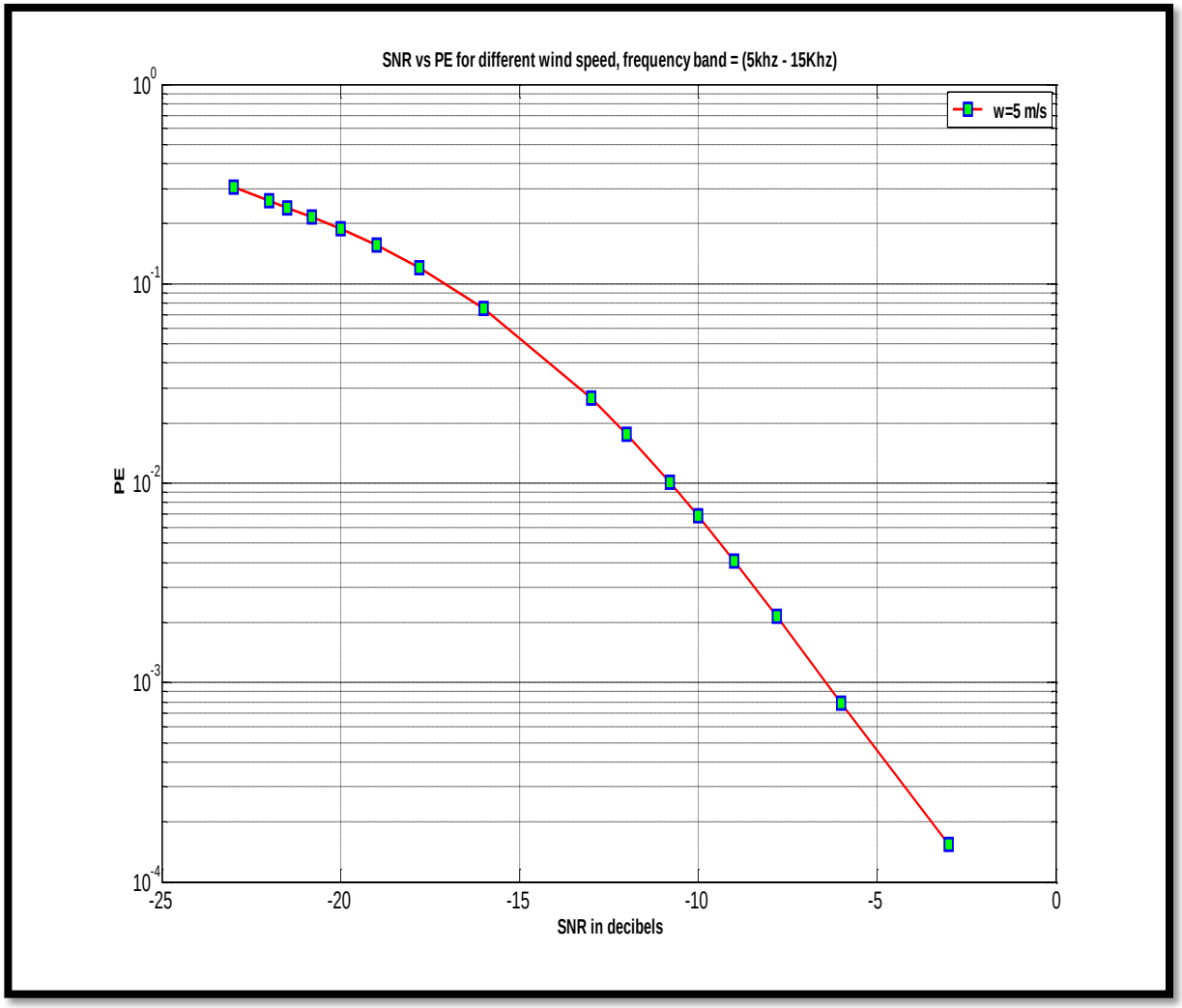

Figure 6.5: Probability of error of CSK for w = 5 m/s.

6.4 WIND SPEED = 7 m/s

At wind speed of 7 m/s, or 25.2 Km/hr the wave activity is very important. This condition does not allow for good performance due to the high value of the noise average power is for a very agitated ocean environment. Equation (3.5) becomes:

$$10\log N_w(f) = 50 + 7.5\sqrt{7} + 20\log f - 40\log(f + 0.4)\,. \qquad (6.5)$$

Figure 6.6 represents the probability of error (P_e) vs SNR

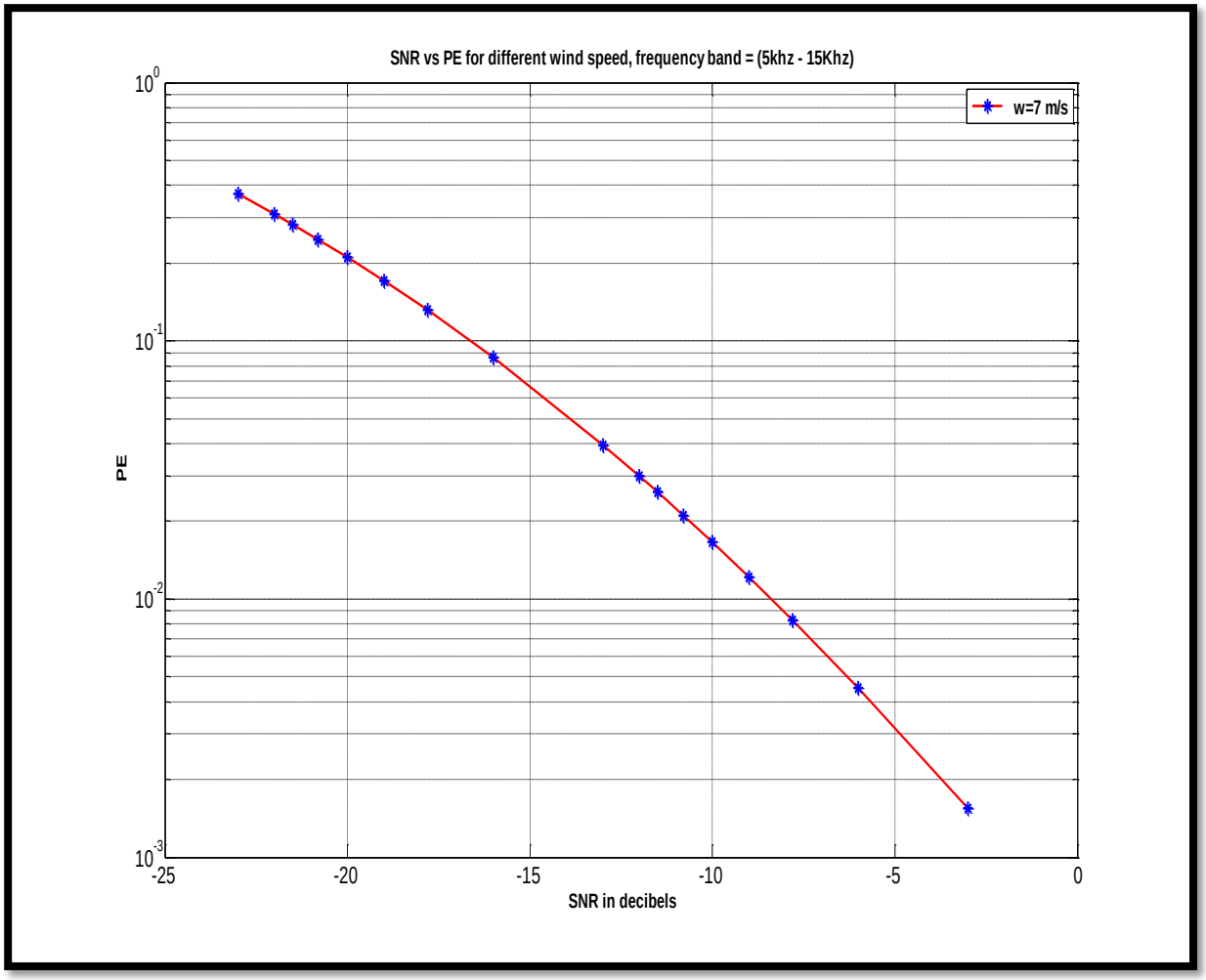

Figure 6.6: Probability of error of CSK for w = 7 m/s.

6.5 COMPARISON OF RESULTS FOR THE DIFFERENT WIND SPEED

In this section, we compare and discuss all the results. The BER curves for the various speed of wind are shown in Figure 6.7.

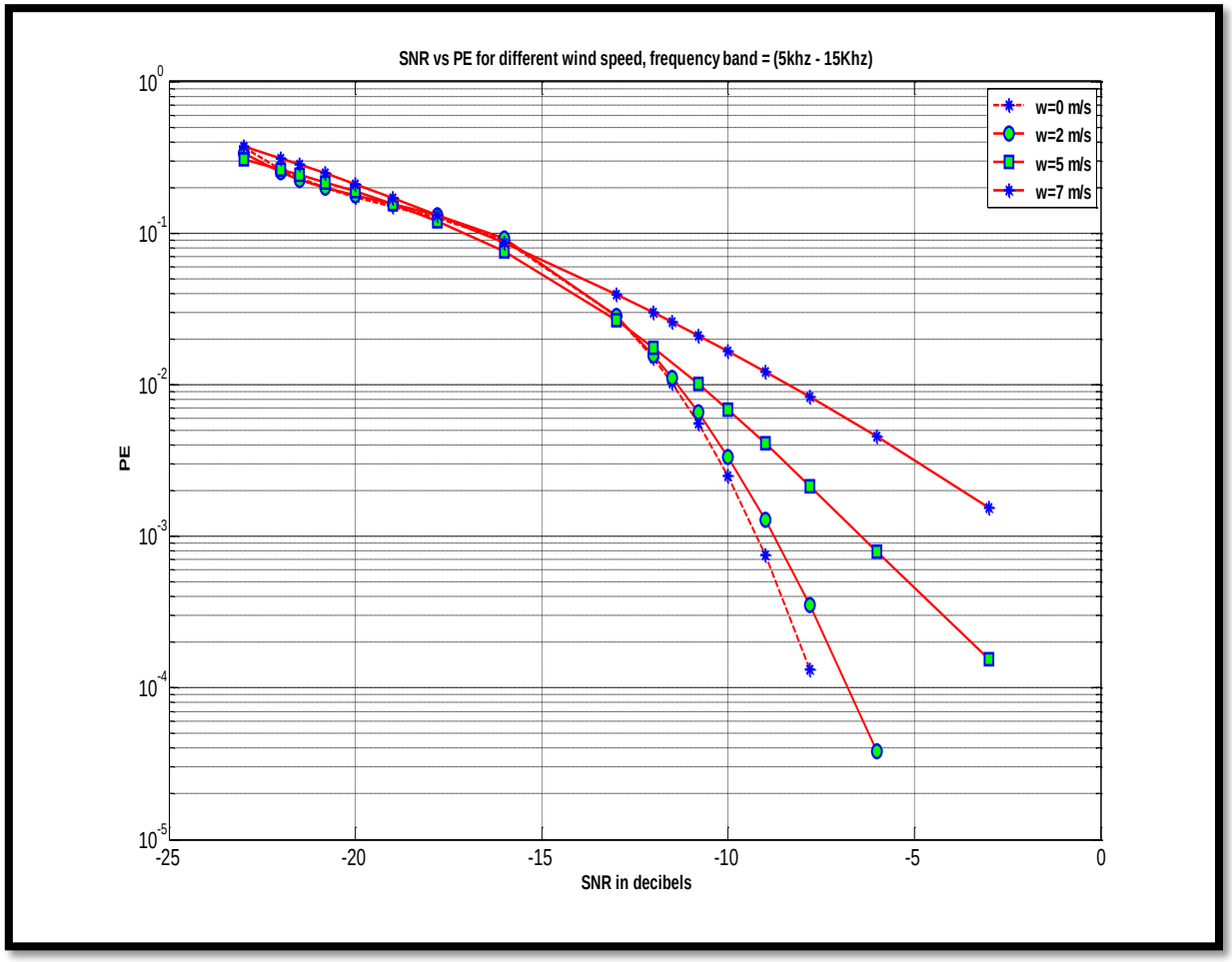

Figure 6.7: BER of CSK for different wind speeds.

The performance of CSK degrades gracefully as the wind speed increases. We can see from figure 6.7 that for a BER of 10^{-3}, The required SNR for w = 0 m/s wind speed is approximately $2\ dB$ smaller than for m/s wind and $4\ dB$ smaller than for 5 m/s. The presence of high winds does not provide satisfactory data transmission but these are

not everyday conditions of the sea. Even in bad weather conditions, CSK can be used to transmit data. Certainly not at a fast rate but may be good enough for short and simple messages.

7. CONCLUSION AND SUGGESTIONS FOR FUTURE WORK

Chirp-Slope Keying (CSK) is a good modulation scheme for underwater communication. In our thesis, we presented the fundamentals of underwater wireless communications, we also presented the different components of the ocean environment and how they affect sound signal propagation from a transmitter to a receiver. Using data collected from NOAA (see appendix E), we were able to mathematically generate a model for CSK simulation using Simulink. We used different wind speeds to estimate the performance of CSK modulation. Our receiver model used a correlation receiver. The BER curves for the different conditions showed that CSK was feasible even at high-wind conditions in the ocean.

In this research, direct path transmission was assumed; future work can improve our model by adding Rayleigh fading (fading of a signal according to Rayleigh distribution) as well as Doppler Effect (change in the observed frequency of a sound signal when the source and observer are in motion relative to each other). Also, future research can investigate data synchronization. It is imperative to distinguish between the presence of a signal and that of noise only. This is an issue that has to be dealt with because we assumed that synchronization was not a problem in our thesis. However, this is not really true; system can become unsynchronized in actual conditions due to internal or external factors. That is what makes it an interesting topic to work on.

8. REFERENCES

[1] E.K Bourgeois and K. Jovanovich, “CSK Modulation for Underwater Communications, Final Report” 44 CLIN 0004, December 2008

[2] M. Stojanovic, “On the relationship between capacity and distance in an underwater acoustic communication channel,” *Mobile Computing and Communications Review*, Volume 11, Number 4, pp. 34-43, September 2006.

[3] M.C. Domingo, “Overview of channel models for underwater wireless communication networks,” *Physical Communication 1*, pp. 163-182, January 2008.

[4] X. Rong Li, “Probability, random signals, and statistics,” CRC press, 1999.

[5] B. Sklar, “Digital communications: fundamentals and applications,” Prentice Hall 1991.

[6] S.K. Mitra, “Digital Signal Processing: a computer based approach, third edition,” McGraw Hill, 2005.

[7] S.M Kay “Fundamentals of statistical signal processing: detection theory,” Prentice Hall, 1998.

[8] J.A.Rice, ”Sea Web acoustic communication and navigation networks,” in Proc. *International Conference on Underwater Acoustic Measurements*, July 2005.

[9] S.Toumpis and A.Goldsmith, “Capacity regions for wireless ad hoc networks,” *IEEE Trans.Wireless Commun.*, vol.2, pp.736-748, July 2003.

[10] H.M.Kwon and T.Birdsal, ‘Channel capacity in bits per Joule,” *IEEE J.Oceanic Eng.*, vol.11, No.1, pp.97-99, Jan. 1986.

[11] H.Leinhos, “Capacity calculations for rapidly fading communications channels,”*IEEE J.Oceanic Eng.*, vol.21, No.2, pp.137-142, Apr.1996.

[12] L.Berkhovskikh and Y.Lysanov, *Fundamentals of Ocean Acoustics* ” New York:Springer, 1982.

[13] R.Coates, *Underwater Acoustic Systems*, New York: Wiley, 1989.

[14] J.G.Proakis, *Digital Communications*, New York: Mc-Graw Hill, 2001.

[15] R. Galvin, R.F.W Coates, Analysis of the performance of an underwater acoustic communication system and comparison with stochastic model, IEEE Oceans'94, Brest, France, 1994, pp. III/478_III/482.

[16] X. Geng, A. Zielinski, An eigenpath underwater acoustic communication channel model, in: Proc. OCEANS, MTS/IEEE, `Challenges Our Changing Global Environment' Conf., 2, Oct. 1995, pp. 1189_1196.

[17] M. Chitre, A high-frequency warm shallow water acoustic communications channel model and measurements, Journal of the Acoustical Society America 122 (5) (2007) 2580_2586.

[18] J.W. Caruthers, Fundamentals of Marine Acoustics, in: Elsevier's Oceanographic Series, vol. 18, Elsevier Scientific Publishing Co, Amsterdam, The Netherlands, 1977.

[19] L.E. Kinsler, A.R. Frey, A.B. Coppens, J.V. Sanders, Fundamentals of Acoustics, 4th ed., John Wiley & Sons cop, New York, 2000.

[20] H. Medwin, C.S. Clay, Fundamentals of Acoustical Oceanography, Academic Press, San Diego, 1997.

[21] M. Schulkin, H.W. Marsh, Sound absorption in sea water, Journal of the Acoustical Society of America 34 (1962) 864_865.

[22] F.H. Fisher, V.P. Simmons, Sound absorption in sea water, Journal of the Acoustical Society of America 62 (1977) 558_564.

[23] R.E. Francois, G.R. Garrison, Sound absorption based on ocean measurements: Part I: Pure water and magnesium sulfate contributions, Journal of the Acoustical Society of America 72 (3) (1982) 896_907.

[24] R.E. Francois, G.R. Garrison, Sound absorption based on ocean Measurements: Part II: Boric acid contribution and equation for total absorption, Journal of the Acoustical Society of America 72 (6) (1982) 1879_1890.

[25] M.A. Ainslie, J.G. McColm, A simplified formula for viscous and chemical absorption in sea water, Journal of the Acoustical Society of America 103 (1998) 1671_1672.

[26] L.M. Brekhovskikh, Y.P. Lysanov, Fundamentals of Ocean Acoustics, 3rd ed.,Springer, New York, 2003.

[27] L.E Simanjuntak, “A novel chirp slope keying modulation scheme for underwater communication” Thesis submitted to the University of New Orleans Graduate School, December 2004.

[28] http://www.ncddc.noaa.gov/website/GOM_Portal/viewer.htm.

9. APPENDICES

9.1 APPENDIX A

Table 9.1 – **Wind speed = 0 $\mathbf{m/s}$ table for simulation with AWGN and colored noise**

SNR	Variance	Number of bits sent for 10 errors	BER
100	-23.0103	**29**	0.3448
80	-22.0412	37	0.2703
70	-21.4613	37	0.2703
60	-20.7918	51	0.1961
50	-20	64	0.1563
40	-19.0309	72	0.1389
30	-17.7815	76	0.1316
20	-16.0206	113	0.0885
10	-13.0103	304	0.03289
8	-12.0412	710	0.01408
7	-11.4613	930	0.01075
6	-10.7918	2162	0.004625
5	-10	4185	0.002389
4	-9.0309	1.13E+04	0.0008855
3	-7.78151	7.99E+04	0.0001252
2	-6.0206	9.34E+05	1.07E-05

9.2 APPENDIX B

Table 9.2 – **Wind speed = $2\ \mathrm{m/s}$ table for simulation with AWGN and colored noise**

SNR	Variance	Number of bits sent for 10 errors	BER
100	-23.0103	**33**	**0.303**
80	-22.0412	37	0.2703
70	-21.4613	37	0.2703
60	-20.7918	50	0.2
50	-20	64	0.1563
40	-19.0309	72	0.1389
30	-17.7815	72	0.1389
20	-16.0206	113	0.0885
10	-13.0103	273	0.03663
8	-12.0412	710	0.01408
7	-11.4613	866	0.01155
6	-10.7918	1627	0.006146
5	-10	3636	0.00275
4	-9.0309	7355	0.00136
3	-7.78151	2.59E+04	0.0003861
2	-6.0206	2.70E+05	3.71E-05

9.3 APPENDIX C

Table 9.3 – **Wind speed = $5\ \mathrm{m/s}$ table for simulation with AWGN and colored noise**

SNR	Variance	Number of bits sent for 10 errors	BER
100	-23.0103	**32**	**0.3125**
80	-22.0412	37	0.2703
70	-21.4613	37	0.2703
60	-20.7918	51	0.1961
50	-20	64	0.1563
40	-19.0309	72	0.1389
30	-17.7815	76	0.1316
20	-16.0206	113	0.0885
10	-13.0103	273	0.03663
8	-12.0412	710	0.01408
7	-11.4613	390	0.02564
6	-10.7918	968	0.01033
5	-10	1638	0.006124
4	-9.0309	2972	0.003365
3	-7.78151	5658	0.001767
2	-6.0206	8130	0.00123

9.4 APPENDIX D

Table 9.4 – **Wind speed = 7m/s table for simulation with AWGN and colored noise**

SNR	Variance	Number of bits sent for 10 errors	BER
100	-23.0103	**29**	**0.3448**
80	-22.0412	37	0.2703
70	-21.4613	37	0.2703
60	-20.7918	41	0.2439
50	-20	51	0.1961
40	-19.0309	59	0.1695
30	-17.7815	59	0.1695
20	-16.0206	100	0.1
10	-13.0103	134	0.07463
8	-12.0412	263	0.03802
7	-11.4613	388	0.02577
6	-10.7918	451	0.02217
5	-10	808	0.01238
4	-9.0309	1192	0.008389
3	-7.78151	2225	0.004494
2	-6.0206	2869	0.003486

9.5 APPENDIX E

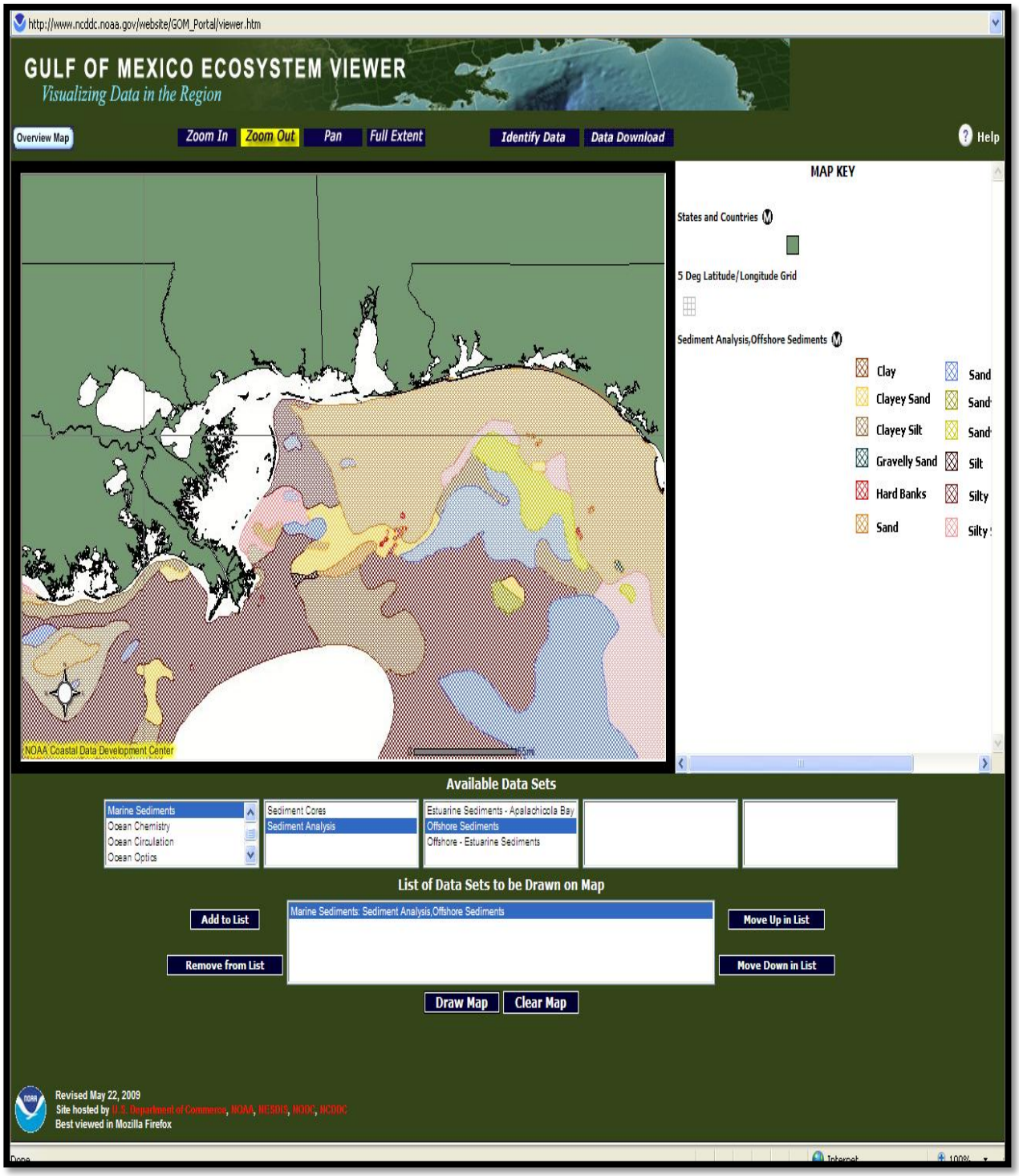

Figure 6.8: Mississippi Gulf coast shallow water sediment Analysis [28].

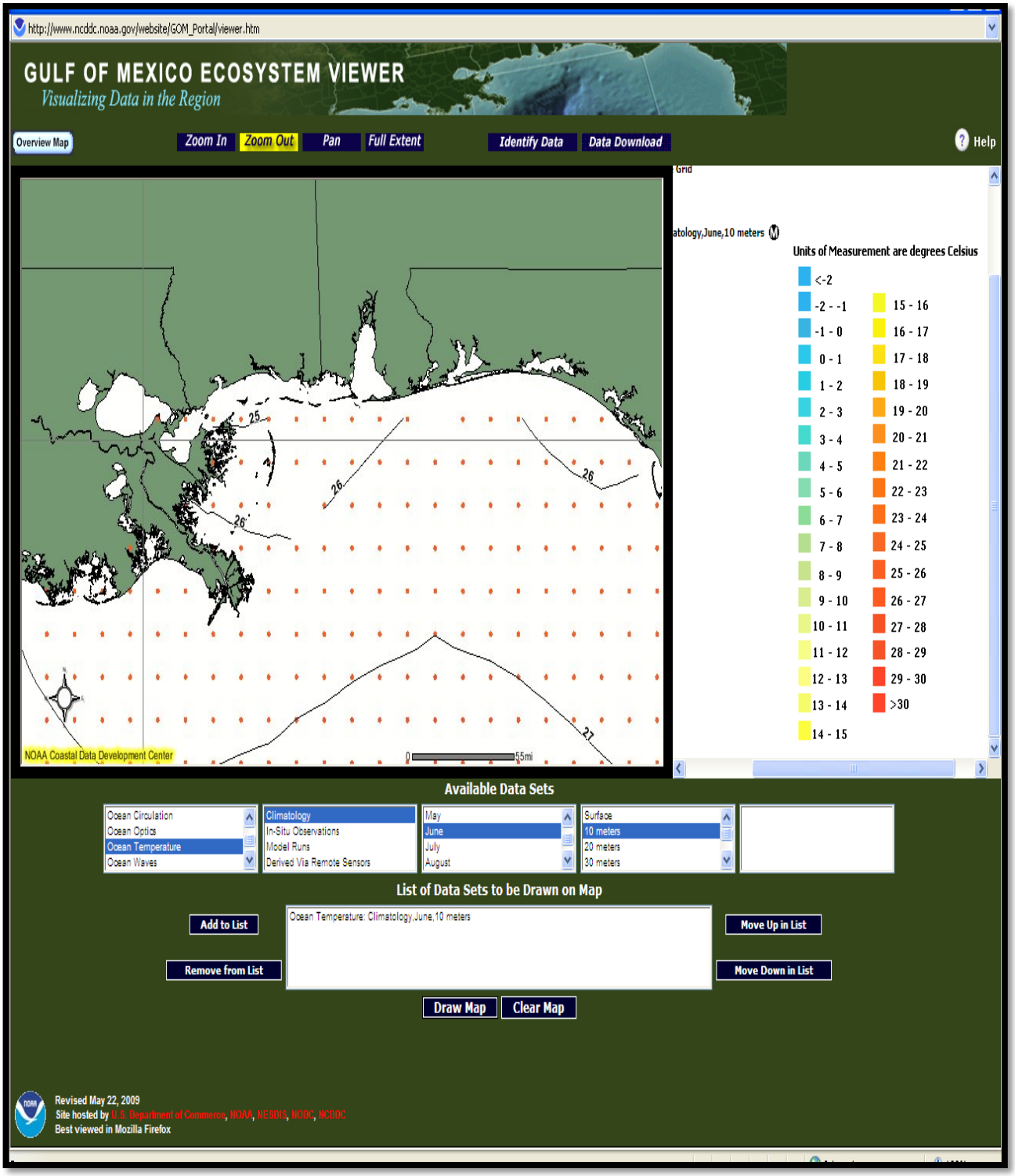

Figure 6.9: Mississippi Gulf coast shallow water temperature [28].

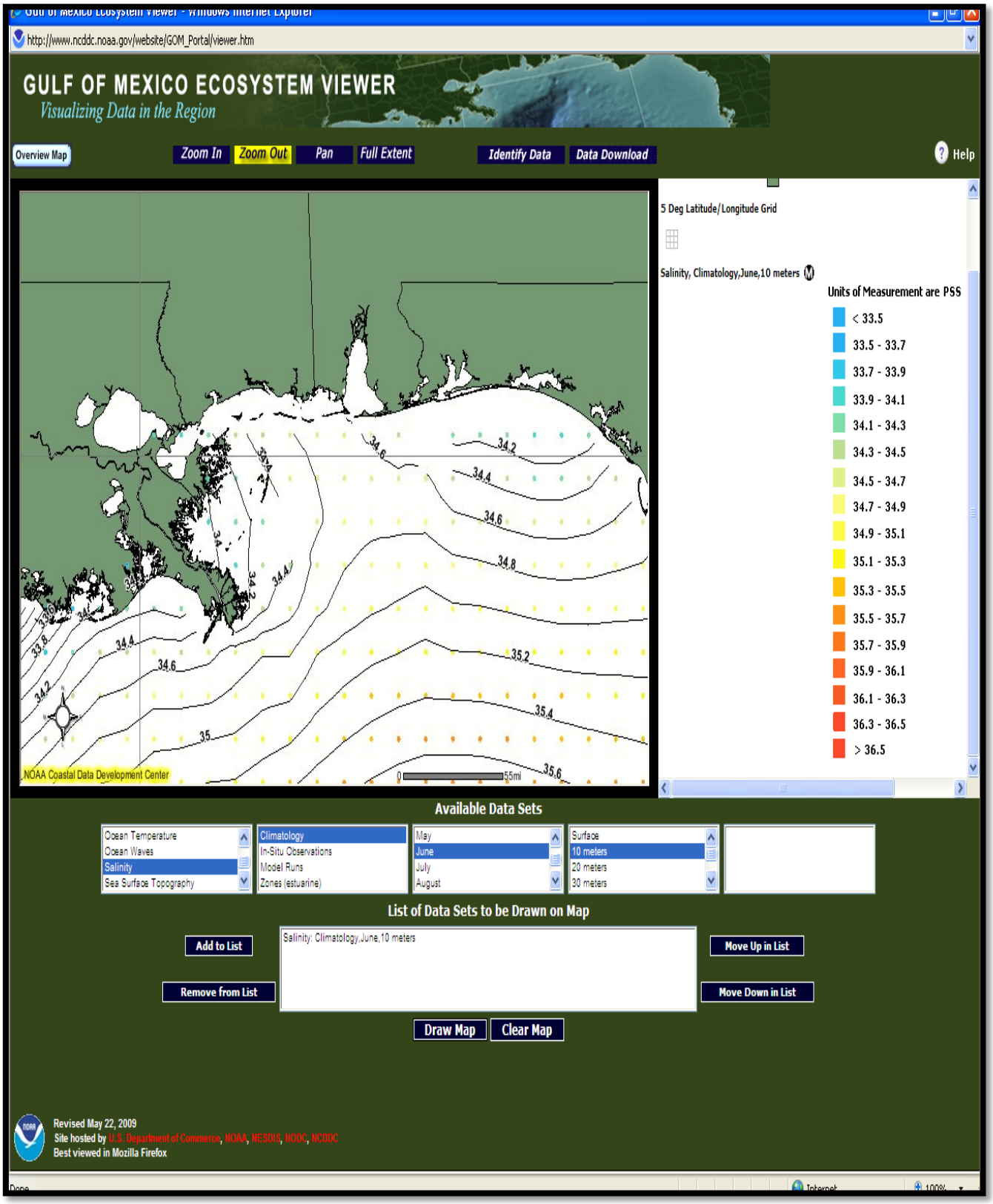

Figure 6.10: Mississippi Gulf coast shallow water salinity [28].

Table 9.5 – **Absorption coefficient using NOOA data [28].**

Frequency f (kHz)	**5**	**8**	**10**	**15**
Temperature T (degree Celsius)	25.86	25.86	25.86	25.86
Salinity S (mg/l)	34.88	34.88	34.88	34.88
Wind Speed w (m/s)	10	10	10	10
Speed of sound c (m/s)	1539.1	1539.1	1539.1	1539.1
Boric Acid Component A_1 (s/m)	0.0279	0.0279	0.0279	0.0279
Magnesium sulfate Component A_2 (s/m)	0.8459	0.8459	0.8459	0.8459
Pure water viscosities A_3	1.858 e -4	1.858 e -4	1.858 e -4	1.858 e -4
Relaxation Frequency for Boric f_1 Acid (kHz)	1.9620	1.9620	1.9620	1.9620
Relaxation Frequency for Magnesium sulfate f_2 (kHz)	178.698	178.698	178.698	178.698
Depth pressure for Boric Acid P_1 (Pa)	1	1	1	1
Depth pressure for Magnesium P_2 sulfate (Pa)	0.9986	0.9986	0.9986	0.9986
Depth pressure for pure water P_3 (Pa)	0.9996	0.9996	0.9996	0.9996
Absorption Coefficient α	0.5983	0.6055	0.6204	0.6354

9.6 APPENDIX F

MATLAB CODE FOR ABSORPTION COEFFICIENT S-FUNCTION

```
function [sys,x0,str,ts] = absorption(t,x,u,flag)
%TIMESTWO S-function whose output is two times its input.
%   This M-file illustrates how to construct an M-file S-function that
%   computes an output value based upon its input.  The output of this
%   S-function is two times the input value:
%
%   Copyright 1990-2007 The MathWorks, Inc.
%   $Revision: 1.7.2.1 $

%
% Dispatch the flag. The switch function controls the calls to
% S-function routines at each simulation stage of the S-function.
%
D=2;
switch flag,
  %%%%%%%%%%%%%%%%%%
  % Initialization %
  %%%%%%%%%%%%%%%%%%
  % Initialize the states, sample times, and state ordering strings.
  case 0
    [sys,x0,str,ts]=mdlInitializeSizes;

  %%%%%%%%%%%
  % Outputs %
  %%%%%%%%%%%
  % Return the outputs of the S-function block.
  case 3
    sys=mdlOutputs(t,x,u,D);

  %%%%%%%%%%%%%%%%%%%
  % Unhandled flags %
  %%%%%%%%%%%%%%%%%%%
  % There are no termination tasks (flag=9) to be handled.
  % Also, there are no continuous or discrete states,
  % so flags 1,2, and 4 are not used, so return an emptyu
  % matrix
  case { 1, 2, 4, 9 }
    sys=[];

  %%%%%%%%%%%%%%%%%%%%%%%%%%%%%%%%%%%
  % Unexpected flags (error handling)%
  %%%%%%%%%%%%%%%%%%%%%%%%%%%%%%%%%%%
  % Return an error message for unhandled flag values.
  otherwise
    DAStudio.error('Simulink:blocks:unhandledFlag', num2str(flag));

end
```

```
% end timestwo

%
%=============================================================================
=
% mdlInitializeSizes
% Return the sizes, initial conditions, and sample times for the S-function.
%=============================================================================
=
%
function [sys,x0,str,ts] = mdlInitializeSizes()

sizes = simsizes;
sizes.NumContStates  = 0;
sizes.NumDiscStates  = 1;
sizes.NumOutputs     = 1;  % dynamically sized
sizes.NumInputs      = 1;  % dynamically sized
sizes.DirFeedthrough = 1;   % has direct feedthrough
sizes.NumSampleTimes = 1;

sys = simsizes(sizes);
str = [];
x0  = ones(sizes.NumDiscStates,1);
ts  = [-1 0];   % inherited sample time

% end mdlInitializeSizes

%
%=============================================================================
=
% mdlOutputs
% Return the output vector for the S-function
%=============================================================================
=
%
function sys = mdlOutputs(t,x,u,Ab)

Co=10;
cl=512;                     % number of samples
F=[15:-10/cl:5+(10/cl)];
Z=10;                      %Depth of water in meter
T=25.86;                   %Temperature in degree Celcius
S=36.88;                   %Salinity
w=0;                       % speed of wind in m/s
C=1412 + 3.21*T + 1.19*S + 0.0167*Z;
A1=(8.68/C)*10^(0.78*7.3-5);                % Boric Acid Component
A2=21.44*(S/C)*(1+0.025*T);                % Magnesium Sulfate Component
A3=(3.964*10^-4)-(1.146*10^-5)*T + (1.45*10^-7)*T^2 -(6.5*10^-10)*T^3;
                                                % Pure Water Viscosities
F1=2.8*((S/35)^0.5)*10^(4-1245/(273+T)); % Relaxation Frequency for Boric
                                          %Acid in khz
F2=(8.17*10^(8-1990/(273+T)))/(1+0.0018*(S-35));    % Relaxation Frequency
                                                    %for Magnesium Sulfate
P1=1;                      % Depth pressure for Boricc Acid
P2=1-(1.37*10^-4)*Z+(6.2*10^-9)*Z^2;                    % Depth pressure
                                                    %for Magnesium sulfate
```

```
P3=1-(3.83*10^-5)*Z+(4.9*10^-10)*Z^2;                % Depth pressure for
                                                      %Pure Water
A=((A1*P1*F1.*F.*F)/(F.*F+F1*F1))+((A2*P2*F2.*F.*F)/(F.*F+F2*F2))...
                                  +A3*P3.*F.*F; %Absorption coefficient in db
Ab=10.^(A./10)    ;                 %Absorption Coefficient

for n=1:cl
sys = u / Ab(1,n);
end
```

9.7 APPENDIX G

MATLAB CODE FOR UNDERWATER NOISE S-FUNCTION

```
function [sys,x0,str,ts] = UP(t,x,u,flag)
%TIMESTWO S-function whose output is two times its input.
%   This M-file illustrates how to construct an M-file S-function that
%   computes an output value based upon its input.  The output of this
%   S-function is two times the input value:
%

%   Copyright 1990-2007 The MathWorks, Inc.
%   $Revision: 1.7.2.1 $

%
% Dispatch the flag. The switch function controls the calls to
% S-function routines at each simulation stage of the S-function.
%
D=2;
switch flag,
  %%%%%%%%%%%%%%%%%%
  % Initialization %
  %%%%%%%%%%%%%%%%%%
  % Initialize the states, sample times, and state ordering strings.
  case 0
    [sys,x0,str,ts]=mdlInitializeSizes;

  %%%%%%%%%%%
  % Outputs %
  %%%%%%%%%%%
  % Return the outputs of the S-function block.
  case 3
    sys=mdlOutputs(t,x,u,D);

  %%%%%%%%%%%%%%%%%%%
  % Unhandled flags %
  %%%%%%%%%%%%%%%%%%%
  % There are no termination tasks (flag=9) to be handled.
  % Also, there are no continuous or discrete states,
  % so flags 1,2, and 4 are not used, so return an emptyu
  % matrix
  case { 1, 2, 4, 9 }
    sys=[];

  %%%%%%%%%%%%%%%%%%%%%%%%%%%%%%%%%%%
  % Unexpected flags (error handling)%
  %%%%%%%%%%%%%%%%%%%%%%%%%%%%%%%%%%%
  % Return an error message for unhandled flag values.
  otherwise
    DAStudio.error('Simulink:blocks:unhandledFlag', num2str(flag));

end

% end timestwo
```

```
%
%==========================================================================
=
% mdlInitializeSizes
% Return the sizes, initial conditions, and sample times for the S-function.
%==========================================================================
=
%
function [sys,x0,str,ts] = mdlInitializeSizes()

sizes = simsizes;
sizes.NumContStates  = 0;
sizes.NumDiscStates  = 1;
sizes.NumOutputs     = 1;  % dynamically sized
sizes.NumInputs      = 1;  % dynamically sized
sizes.DirFeedthrough = 1;   % has direct feedthrough
sizes.NumSampleTimes = 1;

sys = simsizes(sizes);
str = [];
x0  = ones(sizes.NumDiscStates,1);
ts  = [-1 0];   % inherited sample time

% end mdlInitializeSizes

%
%==========================================================================
=
% mdlOutputs
% Return the output vector for the S-function
%==========================================================================
=
%
function sys = mdlOutputs(t,x,u,Ab)

cl=512;                    %Number of samples
%%%%%%%%%%%%%%%%%%%%%%%%%Noise generation%%%%%%%%%%%%%%%%%%%%%%%%%%%%%%%%
F1=5000:1000/51:6000-(1000/51);            %frequency interval of 1000 Hz
F2=6000:1000/51:7000-(1000/51);
F3=7000:1000/51:8000-(1000/51);
F4=8000:1000/51:9000-(1000/51);
F5=9000:1000/51:10000-(1000/51);
F6=10000:1000/51:11000-(1000/51);
F7=11000:1000/51:12000-(1000/51);
F8=12000:1000/51:13000-(1000/51);
F9=13000:1000/52:14000-(1000/52);
F10=14000:1000/52:15000-(1000/52);


Nw1=(2.*(-5.333333333333336 + (-0.04 - 0.00009999999999999999.*5980)...
    .*5980)./ (0.4 + 0.001.*5980).^3)-(2.*(-5.333333333333336 + ...
    (-0.04 - 0.00009999999999999999.*5000).*5000)./ (0.4 + 0.001.*5000).^3);

Nw2=(2.*(-5.333333333333336 + (-0.04 - 0.00009999999999999999.*6980)...
```

```
     .*6980)./ (0.4 + 0.001.*6980).^3)-(2.*(-5.333333333333336 + ...
     (-0.04 - 0.00009999999999999999.*6000).*6000)./ (0.4 + 0.001.*6000).^3);


Nw3=    (2.*(-5.333333333333336 + (-0.04 - 0.00009999999999999999.*7980)...
    .*7980)./ (0.4 + 0.001.*7980).^3)-(2.*(-5.333333333333336 + ...
(-0.04 - 0.00009999999999999999.*7000).*000)./ (0.4 + 0.001.*7000).^3);


Nw4=(2.*(-5.333333333333336 + (-0.04 - 0.00009999999999999999.*8980)...
.*8980)./ (0.4 + 0.001.*8980).^3)-(2.*(-5.333333333333336 + ...
(-0.04 - 0.00009999999999999999.*8000).*8000)./ (0.4 + 0.001.*8000).^3);


Nw5=    (2.*(-5.333333333333336 + (-0.04 - 0.00009999999999999999.*9980)...
 .*9980)./ (0.4 + 0.001.*9980).^3)-(2.*(-5.333333333333336 +...
(-0.04 - 0.00009999999999999999.*9000).*9000)./ (0.4 + 0.001.*9000).^3);


Nw6=    (2.*(-5.333333333333336 + (-0.04 - 0.00009999999999999999.*10980)...
.*10980)./ (0.4 + 0.001.*10980).^3)-(2.*(-5.333333333333336 + ...
(-0.04 - 0.00009999999999999999.*10000).*10000)./ (0.4 + 0.001.*10000).^3);


Nw7=    (2.*(-5.333333333333336 + (-0.04 - 0.00009999999999999999.*11980)...
.*11980)./ (0.4 + 0.001.*11980).^3)-(2.*(-5.333333333333336 +...
(-0.04 - 0.00009999999999999999.*11000).*11000)./ (0.4 + 0.001.*11000).^3);


Nw8=    (2.*(-5.333333333333336 + (-0.04 - 0.00009999999999999999.*12980)...
.*12980)./ (0.4 + 0.001.*12980).^3)-(2.*(-5.333333333333336 +...
(-0.04 - 0.00009999999999999999.*12000).*12000)./ (0.4 + 0.001.*12000).^3);


Nw9=(2.*(-5.333333333333336 + (-0.04 - 0.00009999999999999999.*13980)...
.*13980)./ (0.4 + 0.001.*13980).^3)-(2.*(-5.333333333333336 + ...
(-0.04 - 0.00009999999999999999.*13000).*13000)./ (0.4 + 0.001.*13000).^3);


Nw10=   (2.*(-5.333333333333336 + (-0.04 - 0.00009999999999999999.*14980)...
.*14980)./ (0.4 + 0.001.*14980).^3)-(2.*(-5.333333333333336 +...
(-0.04 - 0.00009999999999999999.*14000).*14000)./ (0.4 + 0.001.*14000).^3);

%%%%%%%%%%%%%%%%%%%%%%%%%%%%%%Generation of Colored noise%%%%%%%%%%%%%%%%%%
wn1=sqrt(Nw1)*randn(1,51);          %white noise generation for first
                                    %frequency interval

wn2=sqrt(Nw2)*randn(1,51);

wn3=sqrt(Nw3)*randn(1,51);

wn4=sqrt(Nw4)*randn(1,51);
```

```
wn5=sqrt(Nw5)*randn(1,51);

wn6=sqrt(Nw6)*randn(1,51);

wn7=sqrt(Nw7)*randn(1,51);

wn8=sqrt(Nw8)*randn(1,51);

wn9=sqrt(Nw9)*randn(1,52);

wn10=sqrt(Nw10)*randn(1,52);

W= [wn1 wn2 wn3 wn4 wn5 wn6 wn7 wn8 wn9 wn10] ;     %Additive colored noise
%%%%%%%%%%%%%%%%%%%%%%%%%%%%%%%%%%%%%%%%%%%%%%%%%%%%%%%%%%%%%%%%%%%%%%%%%%%%
for n=1:cl
sys =u +W(1,n);
end

% end mdlOutputs
```

10. VITA

Brice Zoh was born on January 17, 1983 in Abidjan, Cote d'Ivoire. He is the fifth child of a family of six children. He obtained his University Diploma in Electronics from the National Polytechnic Institute of Yamoussoukro in June 2004. He then graduated from the University of New Orleans with a Bachelor of Science in Electrical Engineering in May 2008. Mr Zoh expects to receive his Master of Science degree in Engineering with concentration in Electrical Engineering, in December 2010.